Since January 2020 Elsevier has created a COVID-19 resource centre with free information in English and Mandarin on the novel coronavirus COVID-19. The COVID-19 resource centre is hosted on Elsevier Connect, the company's public news and information website.

European Journal of Operational Research 304 (2023) 150–168

Contents lists available at ScienceDirect

European Journal of Operational Research

journal homepage: www.elsevier.com/locate/ejor

Stochastics and Statistics

Testing facility location and dynamic capacity planning for pandemics with demand uncertainty

Kanglin Liu[a], Changchun Liu[b], Xi Xiang[c,*], Zhili Tian[d]

[a] School of Traffic and Transportation, Beijing Jiaotong University, Beijing, 100044, China
[b] Institute of Operations Research & Analytics, National University of Singapore, 117602, Singapore
[c] Department of Industrial Systems Engineering and Management, National University of Singapore, 117602, Singapore
[d] College of Business, Coastal Carolina University, 119 Chanticleer Drive E, Conway, SC, 29526, USA

ARTICLE INFO

Article history:
Received 14 February 2021
Accepted 16 November 2021
Available online 25 November 2021

Keywords:
OR In disaster relief
Dynamic facility location
Capacity planning
Online convex optimization
Gradient descent

ABSTRACT

The outbreak of coronavirus disease 2019 (COVID-19) has seriously affected the whole world, and epidemic research has attracted increasing amounts of scholarly attention. Critical facilities such as warehouses to store emergency supplies and testing or vaccination sites could help to control the spread of COVID-19. This paper focuses on how to locate the testing facilities to satisfy the varying demand, i.e., test kits, caused by pandemics. We propose a two-phase optimization framework to locate facilities and adjust capacity during large-scale emergencies. During the first phase, the initial prepositioning strategies are determined to meet predetermined fill-rate requirements using the sample average approximation formulation. We develop an online convex optimization-based Lagrangian relaxation approach to solve the problem. Specifically, to overcome the difficulty that all scenarios should be addressed simultaneously in each iteration, we adopt an online gradient descent algorithm, in which a near-optimal approximation for a given Lagrangian dual multiplier is constructed. During the second phase, the capacity to deal with varying demand is adjusted dynamically. To overcome the inaccuracy of long-term prediction, we design a dynamic allocation policy and adaptive dynamic allocation policy to adjust the policy to meet the varying demand with only one day's prediction. A comprehensive case study with the threat of COVID-19 is conducted. Numerical results have verified that the proposed two-phase framework is effective in meeting the varying demand caused by pandemics. Specifically, our adaptive policy can achieve a solution with only a 3.3% gap from the optimal solution with perfect information.

1. Introduction

In 2020, coronavirus disease 2019 (COVID-19) has resulted in large economic losses, and the corresponding damage continues to escalate. As of January 26, 2021, more than 100 million cases have been confirmed worldwide (CNN, 2021). In addition to COVID-19, other epidemic diseases have also caused astonishing damage to economic and social development, including the 2014–2016 Ebola virus disease, which led to more than 10,000 deaths in West Africa (CDC, 2016); the novel swine-origin influenza A (H1N1) virus, which was first discovered in 2009 and caused tens of millions of confirmed cases and 12,469 deaths in the United States (CDC, 2019); and the mosquito-borne Zika virus (ZIKV), which has affected 72 countries and territories, causing more than 500 thousand locally acquired cases by September 1, 2016, in the Americas alone (Duong, Dussart, & Buchy, 2017). Such infectious diseases have remained among the top causes of death globally.

In practice, governments and organizations have taken many measures to address the spread of epidemic diseases. Expanding access to testing is of great importance to the general public. With the rapid spread of the epidemic, testing is central to planning response activities in all countries during and after the pandemic. Accurate, effective, and efficient testing can lead to early outbreak detection, which will allow health authorities to quickly isolate and treat infected patients, guide people to consciously perform social distancing, and guide policymakers in lockdown policies of certain areas/activities if needed. Hence, to keep the pandemic under control or prepare for the next wave, a well-planned testing strategy is necessary for both disease prevention and intervention. Establishing such a testing system involves not only locating testing centers or assigning people to the testing facilities but also distributing resources, e.g., test kits, to test centers while considering potential demand uncertainty for testing.

* Corresponding author.
E-mail addresses: klliu@bjtu.edu.cn (K. Liu), oralc@nus.edu.sg (C. Liu), isexiang@nus.edu.sg (X. Xiang), ztian@coastal.edu (Z. Tian).

https://doi.org/10.1016/j.ejor.2021.11.028
0377-2217/

In fact, large-scale emergencies have already attracted significant attention from academia in recent decades. Tomasini & Van Wassenhove (2009) addressed the life cycle of disaster management and included four phases, i.e., *mitigation*, *preparedness*, *response*, and *rehabilitation*. *Mitigation* represents the proactive social components of emergencies, which are composed of laws and restrictions that can help to increase resilience and decrease vulnerability under the threat of disasters. *Preparedness* is a long-lasting and structured decision process that determines the response mechanisms to counter factors that society has not been able to mitigate; for example, cities have fire departments to attend to the relief needs and execute regulations associated with fire safety. *Response* is related to the acts of attending to disasters; this happens after the initial outbreak, such as transportation of emergency supplies, location-relocation of temporary shelters, and evacuation of affected communities. *Rehabilitation* comes after *response* and helps victims restore normality. As stated by Tomasini & Van Wassenhove (2009), the middle steps, *preparedness* and *response*, fall into the scope of disaster logistics, which also represent our research focus. Before disasters, much research focused on prepositioning relief supplies (Rawls & Turnquist, 2010; Velasquez, Mayorga, & Özaltın, 2020; Wenjun, Shu, Jia, Song, & Miao, 2018), locating critical distribution/medical facilities (Liu, Li, & Zhang, 2019; Mostajabdaveh, Gutjahr, & Salman, 2019), building fortifications of critical infrastructures (Liberatore, Scaparra, & Daskin, 2011; Parajuli, Kuzgunkaya, & Vidyarthi, 2021), etc. In the response phase, research topics such as relocating patients/communities (Mills, Argon, & Ziya, 2018; Xu, Qiu, Yang, Lu, & Chen, 2020), adjusting capacities (Alem et al., 2021), resource allocation (Yu, Yang, Miao, & Zhang, 2019; Yu, Zhang, Yang, & Miao, 2018), and evacuation (Regnier, 2008; Wang, 2020) are being further investigated. Our research belongs to the category of studies on jointly optimizing the pre- and post-humanitarian operations in a single program, which are more complex (Alem et al., 2021; Charles, Lauras, Wassenhove, & Dupont, 2016; Jabbarzadeh, Fahimnia, & Seuring, 2014; Vatsa & Jayaswal, 2021). After the outbreak of COVID-19, more researchers began to focus on optimizing related operations with respect to pandemics; interested readers can refer to a recent review paper Queiroz, Ivanov, Dolgui, & Wamba (2020) for more details.

In our study, the first problem is where to locate testing facilities and how to design their capacities during the preparedness phase (i.e., how many test kits they should receive daily and how to decide staffing levels in each facility). Faced with dynamic and uncertain demand volumes, as well as the geographical layout of facility candidates and demand sites, researchers have conducted a number of studies on how to locate retail stores, optimize inventory and production, and manage stock levels as demand for products fluctuates by season (Basciftci, Ahmed, & Shen, 2021b; Shen, Zhan, & Zhang, 2011). Among them, many focus on the resilience and reliability of facility locations under uncertain demand and disruptions using stochastic or robust optimization approaches. Establishing an operational system for epidemic resource distribution presents a very similar set of challenges but under unknown disease spread and human behavioral uncertainties. In this study, we present a comprehensive framework to optimize the locations of testing centers, their capacities, and shipment amounts in the background of pandemics. As the provided framework is presented in a generic form, it aims to address various resource allocation problems during different phases of a pandemic by a stochastic programming (SP) approach for different scenarios in practice. We formulate the first-stage phase into a *sample average approximation* (SAA) formulation to meet predetermined fill-rate requirements. The greatest challenge of SAA is to address all the scenarios simultaneously. To overcome this difficulty, we adopt an online gradient descent algorithm, which constructs a near-optimal approximation for a given Lagrangian dual multiplier. Finally, we develop an online convex optimization-based Lagrangian relaxation approach to solve the first-phase problem.

The second problem involves how to adjust resources dynamically to face varying demand caused by pandemics during the response phase. The demand for large-scale emergencies such as COVID-19 fluctuates significantly with time. Taking the situation in China as an example, *the State Council Information Office of the People's Republic of China* announced five stages of fighting COVID-19. In the second stage, the peak value of newly confirmed cases on the Chinese mainland reached 15,152 on February 12, 2020. Since April 29, 2020, the Chinese government began to focus on sporadic cases and case clusters in some locations, and inbound cases were also generally under control (China's State Council Information Office, 2020). Faced with complicated and changeable situations, governments update policies to adapt to the epidemic. For example, Beijing Municipal Health Commission (2020a, 2020b, 2021) announced that the number of official COVID-19 testing facilities increased from 46 (April 15, 2020) to 128 (June 23, 2020) to 252 (January 8, 2021). Therefore, it is beneficial to involve a dynamic setting while performing optimization. As stated in Sheu (2010), a dynamic supply chain network design is essential for emergency logistics planning in disasters.

In the first problem, we generate possible scenarios to describe future demand uncertainty and obtain an initial location and capacity planning strategy at the very beginning. However, the generated scenarios may have zero probability and lead to an unsatisfying solution. Fortunately, the second problem enrolls scenarios that are derived from the online realized demand data, which dynamically adjust the initial decisions and improve the reliability of the overall solution approach.

For the solution approach, the proposed stochastic facility location and dynamic capacity planning problem lies in the scope of sequential decision-making with uncertainty. According to Powell (2016, 2019a, 2019b), the range of related problems, which is so wide that they have been studied by dozens of distinct academic communities, includes the Markov decision process (Puterman, 2014), approximate/adaptive/neurodynamic programming (Bertsekas & Tsitsiklis, 1996; Powell, 2011), SP (Shapiro, Dentcheva, & Ruszczyński, 2014), robust optimization (Ben-Tal, El Ghaoui, & Nemirovski, 2009) and online learning (Albers, 2003). However, each community develops tailored techniques to address specific problems, and the technique is very likely to be inefficient under different settings. Powell (2016) identified four classes of policies that span all the approaches and claimed that any solution to a sequential decision problem consisted of one or a hybrid of the four classes. Among the aforementioned communities, the Markov decision process (MDP) and SP are two major modeling approaches that have been used in stochastic dynamic capacity planning (Basciftci, Ahmed, & Gebraeel, 2021a), and review papers on strategic capacity planning, such as Martínez-Costa, Mas-Machuca, Benedito, & Corominas (2014); Sabet, Yazdani, Kian, & Galanakis (2020); Van Mieghem (2003), are identified for more details.

However, formulating MDP and SP problems requires additional constraints or variables along with the curse of dimensionality and is often computationally intractable (Basciftci et al., 2021a). In the field of MDP, dynamic programming (DP) algorithms, such as value iteration and policy iteration, are well understood for small-scale problems, while approximated dynamic programming (ADP) and approximate linear programming (ALP) restrict the search of the linear span of a small number of features so that larger-scale instances can be solved (Malek, Abbasi-Yadkori, & Bartlett, 2014). According to Martínez-Costa et al. (2014), the preferred procedure for solving dynamic capacity planning models in recent papers is commercial software (such as CPLEX), while in older papers, DP algorithms (Rajagopalan, Singh, & Morton, 1998; Shulman, 1991) were mainly proposed; however, commercial software has evolved. For

SP, SAA is a major technique for dealing with expected values of random variables. Two major drawbacks of SP include the difficulty of identifying representative scenarios and the computational intractability of large-scale problems (Snyder, 2006). Worse still, the SAA method is unlikely to solve problems in a single program, such as our case study with hundreds of enumerated scenarios. Therefore, a method that can capture system properties based on available data and quickly obtain satisfying solutions with a performance guarantee is urgently needed.

In this paper, we employ an online convex optimization (OCO) approach to address the dynamic and stochastic demand during pandemics. The proposed adaptive policy uses one day's prediction to make a decision and is proven to achieve the "target-based optimal solution", i.e., the solution that minimizes the Euclidean distance to any predetermined multiobjective target. When new data become available, the problem is solved repeatedly and is easy to implement. In summary, we focus on testing facility location and dynamic capacity planning problems simultaneously facing varying demands caused by pandemics. The contributions are summarized as follows.

- We propose an easy-to-implement two-phase framework to solve testing facility location and dynamic capacity planning problems facing varying demand caused by pandemics.
- The first phase aims to locate testing facilities and design their capacities using a sample average approximation formulation. An online convex optimization-based Lagrangian relaxation approach is proposed. Specifically, we adopt an online gradient descent algorithm to overcome the difficulty that all scenarios should be addressed simultaneously in each iteration. The proposed approach can construct a near-optimal approximation for a given Lagrangian dual multiplier in polynomial time. Numerical experiments validate the effectiveness of the proposed algorithm.
- The second phase is to dynamically adjust resources facing varying demand caused by pandemics. We design the dynamic allocation policy and adaptive dynamic allocation policy to adjust decisions with respect to varying demands; the latter policy is
  proven to be asymptotically consistent, which means that it can achieve the "target-based optimal solution" when the planning horizon tends to infinity.
- A comprehensive case study with the threat of COVID-19 is conducted, where time series data, demographic data, economic data, and geographic data are collected to reflect real life conditions. Extensive numerical results show the effectiveness of the two-phase approach.

The remainder of this paper is organized as follows. Section 2 presents a thorough literature review of previous research. Section 3 is composed of a problem statement and model formulation. The two-phase solution approach is explained in Section 4. A case study is given in 5. Finally, Section 6 concludes the paper and points out future research directions.

2. Literature review

Since the outbreak of COVID-19, studies related to pandemics have gained increasing amounts of attention; within this body of literature, our study belongs to the stream of studies on emergency facility location and capacity design. To construct a reliable emergency response system, researchers have made efforts to better locate critical facilities, such as emergency medical services (EMS) stations (Beraldi & Bruni, 2009; Liu et al., 2019; Noyan, 2010), temporary shelters (Bayram & Yaman, 2018; Kınay, Kara, Saldanha-da Gama, & Correia, 2018; Mostajabdaveh et al., 2019) or prepositioning facilities (Elçi & Noyan, 2018; Hong, Lejeune, & Noyan, 2015; Ni, Shu, & Song, 2018; Rawls & Turnquist, 2010; Zhang & Li, 2015). Our research focuses on locating testing facilities, which extend the pure strategic location problem to a dynamic setting. Related papers are summarized in Table 1.

A series of papers focused on a static location model, which assumed that the location and the corresponding capacity remain unchanged during the entire horizon regardless of the variations of demand (Jabbarzadeh et al., 2014). Bayram, Tansel, & Yaman (2015) developed a mixed-integer nonlinear program to study the location of shelters and evacuation routes after disasters, where the total evacuation time (a nonlinear function of the flow on segments) is minimized. Kılcı, Kara, & Bozkaya (2015) proposed a mixed-integer linear programming (MILP) model for selecting shelters with area utilization. The model was validated by real data from Kartal, Istanbul, Turkey, and a case study was conducted on the 2011 Van earthquake. Chen & Yu (2016) studied the location of temporary facility locations for the EMS system associated with disaster-reduced demand and transportation infrastructure. The proposed integer programming is solved by Lagrangian relaxation and tested by a case study of New Taipei City. Mostajabdaveh et al. (2019) focused on predisaster strategic decisions, i.e., determining the location and size of emergency facilities in preparation for potential disasters.

Demand fluctuations and variations are important features during pandemics. When demand varies, dynamic facility locations and capacity planning problems can improve system performance by increasing the utilization of resources on hand. Generally, the entire planning horizon is divided into several time periods, and the decisions are made periodically (Melo, Nickel, & Saldanha-Da-Gama, 2009). Dynamic location problems have been extensively studied since the pioneering work of Ballou (1968). We refer interested readers to review papers such as Arabani & Farahani (2012); Nickel & Saldanha-da Gama (2019) for more details on general multiperiod location problems and Martínez-Costa et al. (2014); Sabet et al. (2020); Van Mieghem (2003) for comprehensive surveys on strategic capacity planning. Related to our background, Jabbarzadeh et al. (2014) presented a multiperiod robust network model for blood supply, and the number and location of permanent and temporary facilities, allocation, and inventory collected were optimized. Charles et al. (2016) proposed a two-stage scenario-based multiperiod relief network design model to address finding an optimal warehouse location, prepositioning, and distribution relief problems at a strategic level. Vatsa & Jayaswal (2021) studied the network design of primary health centers in India using a robust capacitated multiperiod maximal cover location model with server uncertainty.

According to Ni et al. (2018), mitigation and preparedness are predisaster relief actions, while response and recovery pertain to postdisaster relief actions; therefore, we generally classify operations before and after emergencies as two separate phases. Most of the aforementioned papers solely optimized a single phase. For static problems, most papers, with only one exception Mostajabdaveh et al. (2019), focused on predisaster strategic decisions, i.e., determining the location and size of emergency facilities in preparation for potential disasters. For dynamic problems, researchers have mainly focused on the dynamic deployment of resources or victims after emergencies, such as relocation of EMS vehicles (Peng, Delage, & Li, 2020), relocating communities (Xu et al., 2020) and optimizing evacuation routes (Regnier, 2008). Studies considering humanitarian operations both pre- and postdisaster simultaneously are limited, and our paper belongs to this category. For example, Mostajabdaveh et al. (2019) developed a scenario-based SP model with demand and disruption uncertainties and characterized the expected outcome (predisaster) and realized outcome (postdisaster) by the so-called ex ante and ex post inequality aversion objectives. Alem et al. (2021) developed a two-stage SP

Table 1
Literature review on facility location and capacity planning strategies in humanitarian logistics.

Paper	Demand	Multi-period	Capacity design	Two-stage	Two-phase		Solution approach	Underlying setting
					pre	post		
Kılcı et al. (2015)	D				✓		Solver	Shelter location
Bayram et al. (2015)	D				✓		Solver	Shelter location & evacuation
Chen & Yu (2016)	D				✓		LR	EMS facility location
Rawls & Turnquist (2010)	U(SP)		✓	✓	✓		LR	Prepositioning of supplies
Bayram & Yaman (2018)	U(SP)			✓	✓		BD	Shelter location & evacuation
Beraldi & Bruni (2009)	U(SP,CC)		✓	✓	✓		BB&He	EMS facility location
Noyan (2010)	U(SP,CC)		✓	✓	✓		He	EMS facility location
Hong et al. (2015)	U(SP,CC)		✓	✓	✓		PA&Solver	Pre-disaster network design
Elçi & Noyan (2018)	U(SP,CC)		✓	✓	✓		BD&BC	Pre-disaster network design
Kınay et al. (2018)	U(SP,CC)				✓		Solver	Shelter location
Mostajabdaveh et al. (2019)	U(SP,CC)			✓	✓	✓	Solver&GA	Shelter location
Ni et al. (2018)	U(RO)			✓	✓		BD	Prepositioning of supplies
Zhang & Li (2015)	U(RO,CC)		✓		✓		BC	EMS facility location
Liu et al. (2019)	U(RO,CC)			✓	✓		Solver	EMS facility location
Jabbarzadeh et al. (2014)	U(RO)	✓		✓	✓	✓	Solver	Blood network design
Charles et al. (2016)	U(SP)	✓		✓	✓	✓	Solver	Relief network design
Peng et al. (2020)	U(SP,CC)	✓	✓	✓		✓	BC	EMS facility location
Alem et al. (2021)	U(SP)	✓	✓	✓	✓	✓	Solver&He	Prepositioning of supplies
Vatsa & Jayaswal (2021)	U(RO)	✓		✓	✓		BD	Primary Health Centers location
This paper	U(SP)	✓	✓	✓	✓	✓	LR-OCO	Testing facilities network design
Demand	D: determinate; U: uncertain; SP: stochastic programming; RO: robust optimization; CC: chance constraint							
Two-phase	pre: pre-disaster; post: post-disaster							
Solution approach	LR: Lagrangian Relaxation; BB: branch and bound; BD: Benders Decomposition GA: genetic algorithm; BC: branch and cut; PA: preprocessing algorithm; He: heuristic OCO: online convex optimization							

model to address the location, capacity, prepositioning, procurement, and assignment decisions during the preparedness and response phases with the social vulnerability index. Like Jabbarzadeh et al. (2014) and Charles et al. (2016), we decide the long-term strategical decisions at the beginning of the planning horizon and adjust the short-term tactical strategies with realized random demand in each time period.

To better characterize the inherent uncertainty and dynamic nature of emergencies, sequential decision-making with uncertainty is the primary solution approach to solve multiperiod dynamic location and capacity design problems. Powell (2011) first hinted at four classes for designing policies in sequential decision problems and extended their earlier thinking by recognizing these four classes into two categories in Powell (2016), i.e., policy search, which includes policy function approximations (PFAs) and cost function approximations (CFAs), and policies based on lookahead approximations, which include policies based on value function approximations (VFAs) and lookahead approximations. Powell (2016, 2019a, 2019b) noted that the aforementioned four classes of policies provide a simple and unified umbrella for problems that arise in stochastic optimization; that is, any solution to a sequential decision problem, such as MDP, SP, robust optimization (RO), and online learning, uses one of the four classes or a hybrid.

Uncertainties over a multiperiod planning horizon are addressed with different methods (Van Mieghem, 2003), such as DP and SP. Shulman (1991) explicitly merged dynamic facility location with capacity expansion and proposed a Lagrangian relaxation-based procedure. Rajagopalan et al. (1998) studied capacity acquisition decisions and their timing to meet customer demand by a DP-based method. Lin, Chen, & Chu (2014), Wang & Nguyen (2017) and Meissner & Senicheva (2018) employed a stochastic DP to analyze the capacity planning problem; however, a large number of states and actions significantly increased the computational burden. Meissner & Senicheva (2018) is the most relevant paper that uses MDP techniques; they examined a multilocation inventory system to optimize inventory transshipment sources, destinations, and the number of units with dynamic and stochastic demand and employed DP introduced by Bellman (1966) to solve small-scaled instances and an ADP approach to find near-optimal policies. According to their results, DP can solve problems to optimality, but it is not able to tackle real-life instances due to the enormous size of the states and decision spaces. Although ADP can obtain a near-optimal solution for real-life cases, the computational time is still unsatisfactory (for instance, the case with 20 facilities and 28 days was solved in 2,059.55 seconds by ADP). As our problem is more complex, MDP-based techniques are not suitable in our setting; compared with Meissner & Senicheva (2018), our extensions can be summarized in the following two aspects. First, in addition to transportation flow and inventory, location is also an important decision variable in our study, while they assumed location as an input parameter. Second, our case study is composed of 66 facility candidates, 333 demand sites, and 250 days, which is much larger than their largest instance (20 facilities and 28 days).

Currently, SP has become a fundamental methodology to address related problems by enumerating the underlying scenarios. Rawls & Turnquist (2010) described a two-stage scenario-based stochastic model with demand uncertainty to determine the location, sizing, and allocation of relief supplies. Bayram & Yaman (2018) extend their earlier work in Bayram et al. (2015) through the consideration of uncertainties in evacuation demand and solve the proposed problem by Benders decomposition. Jin, Ryan, Watson, & Woodruff (2011) and Marín, Martínez-Merino, Rodríguez-Chía, & Saldanha-da Gama (2018) formulated the capacity expansion planning problem with demand uncertainty as a two-stage SP and dynamically determined the capacity expansion or transshipment decisions. Related problems can also be formulated as a multistage mixed-integer SP through a scenario tree. For instance, Singh, Philpott, & Wood (2009) and Yu, Ahmed, & Shen (2021) adopted scenario trees to represent uncertainties in the capacity design and dynamic location problem, and the proposed MILP was solved by Dantzig-Wolfe decomposition and stochastic dual dynamic integer programming, respectively. Notably, a number of papers adopt chance constraints to describe uncertainty, and the computationally intractable chance constraints can be either

reformulated by a series of scenarios using SP (Beraldi & Bruni, 2009; Elçi & Noyan, 2018; Hong et al., 2015; Kınay et al., 2018; Mostajabdaveh et al., 2019; Noyan, 2010) or approximated by partial information via RO (Liu et al., 2019; Zhang & Li, 2015).

In this paper, we formulate a two-stage stochastic program (reformulated by the SAA approach) considering fill-rate constraints to solve our first-phase problem. The main challenge of the SAA approach is that increasing the number of scenarios will lead to an exponential increase in computational complexity, and it may not solve a large-scale instance such as the one that we examine. To overcome this difficulty, we adopt a novel approach by using an online environment where demand arrives over time so that short-term tactical strategies (such as capacity and assignment) can be adjusted once the situation changes, i.e., the OCO technique. The OCO method was first introduced by Zinkevich (2003) and could obtain a near-optimal approximation for a given Lagrangian dual multiplier in polynomial time. For more details about the OCO framework, readers can refer to Cesa-Bianchi & Lugosi (2006); Lyu et al. (2019a); Lyu, Cheung, Teo, & Wang (2019b); Shalev-Shwartz et al. (2011). Because of its theoretical guarantee and computational tractability, the OCO framework has been successfully used in optimization areas such as online ride-matching (Lyu et al., 2019b) and production network optimization (Lyu et al., 2019a); we introduce this advanced algorithm to humanitarian logistics, where a unique and converged step direction is proposed based on the special structure of our problem. Specifically, we implement the online gradient descent algorithm in the Lagrangian relaxation approach to achieve a sublinear regret bound compared with the offline optimization approach.

3. Problem statement

We consider a general multiperiod testing facility location and capacity design problem. The original network is composed of J facility candidates and I demand sites. Total supplies delivered by a single facility should not exceed its current capacity, and a certain demand site can be served by different facilities, i.e., a multi-sourcing assignment setting. The goal of this problem is to identify the optimal location and capacity strategies during the entire time horizon with the objective of minimizing the total operational cost. As demand uncertainty can never be underestimated, we introduce parameter $\boldsymbol{d}$ as representative of random demand. A type-II service level constraint is involved to keep customers satisfied, and unmet demand is strictly penalized in the objective. Service fairness another important issue for planners is achieved by defining the maximum covering distance.

Throughout this paper, we use bold-face letters to denote vectors and matrices, such as $\boldsymbol{d}$; let set $[R] = \{1, 2, \ldots, R\}$ for any positive integer R; and use lower-case letters and upper-case letters to denote input parameters and decision variables, respectively. Notations are summarized as follows.

Parameters

$[J]$	Set of facility candidates, $[J] = \{1, 2, \cdots, J\}$, indexed by j.
$[I]$	Set of demand sites, $[I] = \{1, 2, \cdots, I\}$, indexed by i.
$[T]$	Set of time periods, $[T] = \{1, 2, \cdots, T\}$, indexed by t.
f_j	Fixed construction cost of opening a facility at node j.
a_{jt}	Varying construction cost of investigating one unit of capacity at facility candidate j in period t.
η	Unit transportation cost.
c_{ij}	Travel distance between demand site i and facility candidate j.
p_{it}	Unit penalty cost of unmet demand at demand site i in period t.
$d_i(t)$	Demand at demand site i in period t.
M	Maximum amount of capacity (a large positive number).
β_i	Expected demand fill rate (type-II service level) at demand site i.
$T_{\max}$	Maximum covering distance.
Cov_i	Set of location candidates that can cover demand site i, $\text{Cov}_i = \{j \in [J] \mid c_{ij} \le T_{\max}\}$.
Dem_j	Set of demand sites that could be served by facility j, $\text{Dem}_j = \{i \in [I] \mid c_{ij} \le T_{\text{maximum}}\}$.

Decision variables

X_j	Binary variable; equals 1 if a facility is built at node j and 0 otherwise.
$S_j(t)$	Continuous variable; capacity available of facility j in period t.
$Y_{ij}(t)$	Continuous variable: amount of relief supplies that travels from facility j to demand site i in period t.
$W_i(t)$	Continuous variable; unmet demand of node i in period t.

To ensure that every demand site could obtain prompt relief service with equal probability, we define the maximum distance that demand sites could be covered ($T_{\max}$) and use sets Cov_i and Dem_j to denote responsive service regions. Without loss of generality, the mathematical model is based on the following assumptions:

(a) Facilities are built in the first period with a corresponding initial capacity and are not be destroyed later.
(b) Capacity could be adjusted with realizations of time-varying demand.
(c) A dummy period 0 is introduced, where the initial values of $S_j(0) = 0, \forall j \in [J]$.

As building a facility can be expensive and the effect is long-lasting, facilities are unlikely to be destroyed once built; therefore, assumption (a) has been widely used in related studies such as that of Charles et al. (2016); Jabbarzadeh et al. (2014); Vatsa & Jayaswal (2021); Yu & Shen (2020). Nevertheless, decision-makers should respond in a timely manner to demand fluctuations. To this end, assumption (b) finds a cheaper and easier way, where facility capacity could be adjusted by incorporating additional investigation cost (Nickel & Saldanha-da Gama, 2019). Assumption (c) defines the values of auxiliary decision variables to remain consistent.

Essentially, the determinate facility location and capacity configuration problem with perfect information can be formulated as the following MILP.

$$[\text{P1}] \quad \min \quad \sum_{j\in[J]} f_j X_j + \sum_{t\in[T]}\sum_{j\in[J]} a_{jt}\big(S_j(t) - S_j(t-1)\big) + \eta \sum_{t\in[T]}\sum_{i\in[I]}\sum_{j\in[J]} c_{ij} Y_{ij}(t) + \sum_{t\in[T]}\sum_{i\in[I]} p_{it} W_i(t), \tag{1a}$$

$$\text{s.t.} \quad \sum_{j\in \text{Cov}_i} Y_{ij}(t) \ge \beta_i d_i(t), \quad \forall i \in [I], t \in [T], \tag{1b}$$

$$\sum_{j\in \text{Cov}_i} Y_{ij}(t) + W_i(t) \ge d_i(t), \quad \forall i \in [I], t \in [T], \tag{1c}$$

$$\sum_{i\in \text{Dem}_j} Y_{ij}(t) \le S_j(t), \quad \forall j \in [J], t \in [T], \tag{1d}$$

$$S_j(t) \le M X_j, \quad \forall j \in [J], t \in [T], \tag{1e}$$

$$S_j(t) \ge S_j(t-1), \quad \forall j \in [J], t \in [T], \tag{1f}$$

$$X_j \in \{0, 1\}, \quad \forall j \in [J], \tag{1g}$$

(continued on next page)

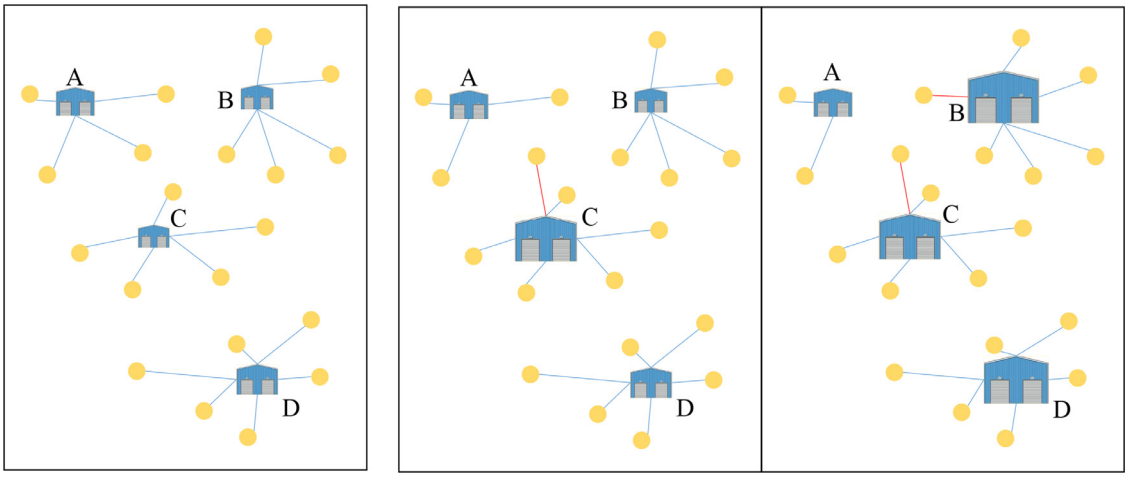

(a) Phase I: Construction ($t = 1$) (b) Phase II: Operations ($t = 2, 3$)

Fig. 1. Sketch of the solution approach (capacity expansion is illustrated by larger facility icons).

$$S_j(t), W_j(t) \geq 0, \quad \forall j \in [J], t \in [T], \tag{1h}$$

$$Y_{ij}(t) \geq 0, \quad \forall i \in [I], j \in [J], t \in [T]. \tag{1i}$$

The objective function (1a) minimizes the total operational cost, which includes construction cost, capacity expansion cost, transportation cost, and penalty cost. Constraints (1b) indicate that supplies allocated to demand site i should be larger than its expected demand with a β_i fill rate (type-II service level). Constraints (1c) are the flow conservation constraint. Constraints (1d) ensure that exported supplies should be no larger than their capacity. Constraints (1e) state that capacity could only be allocated to an open facility. Constraints (1f) to (1i) are integrity and nonnegative constraints.

4. Solution approach

To better fit reality, we divide the problem into two phases: a construction phase and an operational phase (see Fig. 1). Specifically, we first decide the location and initial capacities of the testing facilities, and then infrastructures go into service with capacity expansion decisions in each time period. During the operating process, it is less time-consuming and more convenient to adjust facility capacities facing varying demands. As shown in Fig. 1a, the initial location and capacity strategies are first determined during the construction phase ($t = 1$); in regard to Fig. 1b, which is named the operational phase, capacity adjustment is allowed; for example, the capacity of facility C is enlarged in period 2, and the capacities of facilities B and D are further expanded in period 3. Moreover, assignment policies could also be modified; see the red-colored lines in Fig. 1b.

4.1. Basic idea

Solving problem [P1] requires addressing T time periods simultaneously, which might result in a large-scale MILP. Furthermore, as demand parameter d_{it} is unknown in the initial stage, it is unlikely to obtain a perfect estimation of future demand. To circumvent computational difficulties and compensate for the lack of full information, we propose a two-phase algorithm to solve this problem, which is in line with reality and easy to implement.

- **Phase I (Construction Phase). Location design and capacity initialization:** Determine the location X_j and the initial capacity $S_j(1)$ with predicted demand. During the time horizon, we evaluate future demand by K ($K = T$) predicted samples, which correspond to T different periods, and the k^{th} sample denotes the predicted demand at the corresponding time period. Thus, problem [P1] could be considered a single-period location and capacity design model with K scenarios. We employ a Lagrangian relaxation algorithm to solve the reformulated model, where an OCO technique, namely, online gradient descent, is used to solve the subproblem within each iteration.
- **Phase II (Operational Phase). Dynamic capacity planning:** Determine the capacity increment $\Delta S_j(t)$, allocation schedule $Y_{ij}(t)$, and corresponding decisions $W_i(t)$ dynamically. After observing the revealed demand at time period t, we make capacity planning decisions dynamically, with the objective of minimizing various costs, including varying construction cost of capacity expansion, transportation cost, penalty cost of unmet demands, and satisfying the service level of each demand site.

4.2. Phase I (construction phase): Location design and capacity initialization

In this section, we develop a Lagrangian relaxation algorithm to determine the location design X_j and the initial capacity $S_j(1)$ given expected service level targets. For simplicity, we use S_j to replace $S_j(1)$ in this subsection.

4.2.1. Model formulation

The multiperiod model is first transformed into a single-period model with K demand scenarios $\hat{d}_i(k)$, $k = 1, \cdots, K$. Assume that demand of demand site i follows probability distribution function D_i and lives in an uncertainty set $[D]_i$, i.e., $d_i \sim D_i$, $[D]_i := \{d : d \sim D_i\}$; then, the model can be reformulated as follows:

$$\text{[P2]} \quad \min \quad \sum_{j\in[J]} f_j X_j + \sum_{j\in[J]} \bar{a}_j S_j + \sum_{i\in[I]} \mathbb{E}\left[\eta \sum_{j\in[J]} c_{ij} Y_{ij}(d_i) + \bar{p}_i W_i(d_i)\right], \tag{2a}$$

$$\text{s.t.} \quad \mathbb{E}\left[\sum_{j\in \text{Cov}_i} Y_{ij}(d_i)\right] \geq \beta_i \mathbb{E}_{D_i}[d_i], \quad \forall i \in [I], \tag{2b}$$

$$\sum_{j\in \text{Cov}_i} Y_{ij}(d_i) + W_i(d_i) \geq d_i, \quad \forall i \in [I], d_i \in [D]_i, \tag{2c}$$

$$\sum_{i\in \text{Dem}_j} Y_{ij}(d_i) \le S_j, \quad \forall j \in [J], d_i \in [D]_i, \tag{2d}$$

$$S_j \le MX_j, \quad \forall j \in [J], \tag{2e}$$

$$X_j \in \{0,1\}, \quad \forall j \in [J], \tag{2f}$$

$$S_j, W_j(d_i) \ge 0, \quad \forall j \in [J], d_i \in [D]_i, \tag{2g}$$

$$Y_{ij}(d_i) \ge 0, \quad \forall i \in [I], j \in [J], d_i \in [D]_i. \tag{2h}$$

where $\overline{a}_j$ and $\overline{p}_i$ are the corresponding expected values computed as

$$\overline{a}_j = \frac{\sum_{k=1}^K a_{jk}}{K}, \quad \overline{p}_j = \frac{\sum_{k=1}^K p_{jk}}{K}.$$

4.2.2. Sample average approximation reformulation

Intuitively, it is generally intractable to solve problem [P2] directly with expected terms. To tackle this difficulty, the use of a typical solution approach, SAA, is a popular choice to approximate the expectation terms in the objective and constraints by sampling K demand scenarios $\left\{\hat{d}_i(k)\right\}_{k=1}^K$, where K is a sufficiently large number. For ease of notation, we denote the capacity that facility j allocates to demand site i by $Y_{ij}(k)$ and the unmet demand of customer i by $W_i(k)$ if $d_i = \hat{d}_i(k)$. Then, the reformulated model is summarized as problem [P3].

$$\begin{aligned}[P3] \quad \min \quad & \sum_{j\in[J]} f_j X_j + \sum_{j\in[J]} \overline{a}_j S_j \\ & + \frac{1}{K} \liminf_{K\to\infty} \sum_{i\in[I]} \left[\eta \sum_{j\in[J]} c_{ij} Y_{ij}(k) + \overline{p}_i W_i(k) \right], \end{aligned} \tag{3a}$$

$$\text{s.t.} \quad \liminf_{K\to\infty} \frac{\sum_{k=1}^K \sum_{j\in \text{Cov}_i} Y_{ij}(k)}{\sum_{k=1}^K \hat{d}_i(k)} \ge \beta_i, \quad \forall i \in [I], \tag{3b}$$

$$\sum_{j\in \text{Cov}_i} Y_{ij}(k) + W_i(k) \ge \hat{d}_i(k), \quad \forall i \in [I], k \in [K], \tag{3c}$$

$$\sum_{i\in \text{Dem}_j} Y_{ij}(k) \le S_j, \quad \forall j \in [J], k \in [K], \tag{3d}$$

$$S_j \le MX_j, \quad \forall j \in [J], \tag{3e}$$

$$X_j \in \{0,1\}, \quad \forall j \in [J], \tag{3f}$$

$$S_j \ge 0, \quad \forall j \in [J], \tag{3g}$$

$$W_j(k) \ge 0, \quad \forall j \in [J], k \in [K], \tag{3h}$$

$$Y_{ij}(k) \ge 0, \quad \forall i \in [I], j \in [J], k \in [K]. \tag{3i}$$

4.2.3. Lagrangian reformulation

For problem (P3), we consider its Lagrangian dual formulation by introducing the Lagrangian dual multiplier $\boldsymbol{\lambda}$ in correspondence with the service level constraints, which can be formulated as

$$\begin{aligned}[P4] \quad \max_{\boldsymbol{\lambda}\ge 0} \min \quad & \sum_{j\in[J]} f_j X_j + \sum_{j\in[J]} \overline{a}_j S_j \\ & + \frac{1}{K} \sum_{k=1}^K \sum_{i\in[I]} \left[\eta \sum_{j\in[J]} c_{ij} Y_{ij}(k) + \overline{p}_i W_i(k) \right], \\ & + \sum_{i\in I} \lambda_i \left[\beta_i \sum_{k=1}^K \hat{d}_i(k) - \sum_{k=1}^K \sum_{j\in \text{Cov}_i} Y_{ij}(k) \right] \\ \text{s.t.} \quad & (3c)\text{-}(3i). \end{aligned} \tag{4a}$$

Following the classic paradigm of Nocedal & Wright (2006), problem [P4] could be solved iteratively by minimizing the inner problem regarding original decision variables ($\boldsymbol{X}$, $\boldsymbol{S}$, $\boldsymbol{Y}$, $\boldsymbol{W}$) and maximizing the outer optimization model with respect to the Lagrangian multiplier ($\boldsymbol{\lambda}$). Suppose in the n^{th} iteration with respect to $\boldsymbol{\lambda}$, the inner minimization problem with fixed $\boldsymbol{\lambda}^n$ is [P5].

$$\begin{aligned}[P5] \quad & \phi^n(\boldsymbol{X}, \boldsymbol{S} | \boldsymbol{\lambda} = \boldsymbol{\lambda}^n, \boldsymbol{d} = \hat{\boldsymbol{d}}) \\ & = \min \quad \sum_{j\in[J]} f_j X_j + \sum_{j\in[J]} \overline{a}_j S_j \\ & + \frac{1}{K} \sum_{k=1}^K \sum_{i\in[I]} \left[\eta \sum_{j\in[J]} c_{ij} Y_{ij}(k) + \overline{p}_i W_i(k) \right] \\ & + \sum_{i\in I} \lambda_i^n \left[\beta_i \sum_{k=1}^K \hat{d}_i(k) - \sum_{k=1}^K \sum_{j\in \text{Cov}_i} Y_{ij}(k) \right], \\ \text{s.t.} \quad & (3c)\text{-}(3i). \end{aligned} \tag{5a}$$

4.2.4. Online gradient descent algorithm for a given lagrangian dual multiplier

Define $(\boldsymbol{X}^{n*}, \boldsymbol{S}^{n*})$ as the optimal solution of [P5] when $\boldsymbol{\lambda} = \boldsymbol{\lambda}^n$, i.e., $(\boldsymbol{X}^{n*}, \boldsymbol{S}^{n*}) = \arg\min \phi^n(\boldsymbol{X}, \boldsymbol{S} | \boldsymbol{\lambda} = \boldsymbol{\lambda}^n, \boldsymbol{d} = \hat{\boldsymbol{d}})$. Note that problem [P5] requires addressing all demand scenarios simultaneously and would result in a time-consuming MILP if K is large. Instead of finding $\boldsymbol{X}^{n*}$ and $\boldsymbol{S}^{n*}$ directly, we use an online gradient descent algorithm to develop a feasible capacity profile $\boldsymbol{S}^n(k-1)$, $k \in [K]$ of [P5], and use these to construct a near-optimal approximation of $\boldsymbol{S}^{n*}$. Afterward, $\boldsymbol{X}^{n*}$ could be obtained through a simple injective function $\pi : \mathbb{R}_+^I \to [0,1]^I$, such that

$$\boldsymbol{X}^{n*} = \pi(\boldsymbol{S}^{n*}) = \begin{cases} 1, & \text{if } \boldsymbol{S}^{n*} > 0, \\ 0, & \text{if } \boldsymbol{S}^{n*} = 0. \end{cases} \tag{6}$$

As X_j can always be observed through the injective function π, we only focus on S_j while solving problem [P5].

In accordance with the roadmap of the OCO technique, [P5] only depends on $\hat{d}_i(k)$, $Y_{ij}(k)$ and $W_i(k)$ with fixed capacity profile $\boldsymbol{S}^n(k-1)$ and the corresponding location $\boldsymbol{X}^n(k-1)$, $k \in [K]$. Therefore, we can obtain a decomposed subproblem [P6] by letting $\boldsymbol{\lambda} = \boldsymbol{\lambda}^n$, $\boldsymbol{X} = \boldsymbol{X}^n(k-1)$, $\boldsymbol{S} = \boldsymbol{S}^n(k-1)$ and $\boldsymbol{d} = \hat{\boldsymbol{d}}(k)$.

$$\begin{aligned}[P6] \quad & f_k^n(\boldsymbol{S}^n(k-1), \boldsymbol{\lambda}^n, \hat{\boldsymbol{d}}(k)) \\ & = \min \quad \sum_{i\in[I]} \left[\sum_{j\in[J]} (\eta c_{ij} - \lambda_i^n) Y_{ij}(k) + \overline{p}_i W_i(k) \right], \end{aligned} \tag{7a}$$

$$\text{s.t.} \quad \sum_{j\in \text{Cov}_i} Y_{ij}(k) + W_i(k) \ge \hat{d}_i(k), \quad \forall i \in [I], \tag{7b}$$

$$\sum_{i\in \text{Dem}_j} Y_{ij}(k) \le S_j^n(k-1), \quad \forall j \in [J], \tag{7c}$$

$$W_j(k) \geq 0, \quad \forall j \in [J], \tag{7d}$$

$$Y_{ij}(k) \geq 0, \quad \forall i \in [I], j \in [J] \tag{7e}$$

Based on the dual form of problem [P6], $S_j^n(k)$ could be updated according to the gradient descent direction (find more details in Step 3.2 of Algorithm 1). With fixed λ, we obtain a near-optimal S_j^n after dealing with all K samples. Finally, the entire algorithm terminates whenever $\boldsymbol{\lambda}$ converges.

4.2.5. Procedure of OCO-based lagrangian relaxation

Detailed procedures of the algorithm are presented as follows:

Algorithm 1. OCO-based LR for location design and capacity initialization algorithm.

- **Input**: Demand distribution $\boldsymbol{D}$
- **Output**: Location design $\boldsymbol{X}^*$, capacity initialization $\boldsymbol{S}^*$ and the initial assignment policy $\boldsymbol{Y}^*$.
- **Step 1: Sample generation**. Generate K demand samples $\boldsymbol{d}(k)$ independently according to the distribution of demand $\boldsymbol{D}$, where $k \in [K]$, and K is a sufficiently large number. Arbitrarily sort the K samples into a sequence. In the multiperiod problem, the K samples can use the forecast demand at T time periods directly.
- **Step 2: Initialization.** Solve a deterministic model with the average demand, i.e., $\bar{d}_i = \frac{\sum_{k=1}^K d_{jk}}{K}$, and initialize the location and capacity decisions.

$$[\text{DM}] \quad \min \quad \sum_{j\in[J]} f_j X_j + \sum_{j\in[J]} \bar{a}_j S_j + \sum_{i\in[I]} \eta \sum_{j\in[J]} c_{ij} Y_{ij} + \bar{p}_i W_i, \tag{8a}$$

$$\text{s.t.} \quad \sum_{j\in \text{Cov}_i} Y_{ij} \geq \beta_i \bar{d}_i, \quad \forall i \in [I], \tag{8b}$$

$$\sum_{j\in \text{Cov}_i} Y_{ij} + W_i \geq \bar{d}_i, \quad \forall i \in [I], \tag{8c}$$

$$\sum_{i\in \text{Dem}_j} Y_{ij} \leq S_j, \quad \forall j \in [J], \tag{8d}$$

$$S_j \leq M X_j, \quad \forall j \in [J], \tag{8e}$$

$$X_j \in \{0,1\}, \quad \forall j \in [J], \tag{8f}$$

$$S_j, W_j \geq 0, Y_{ij} \geq 0, \quad \forall i \in [I], j \in [J]. \tag{8g}$$

Assume the optimal solutions of the above DM are $\boldsymbol{X}^*$, $\boldsymbol{S}^*$, and $\boldsymbol{Y}^*$. Set the iteration number $n = 0$, and,

$$\boldsymbol{X}^0 = \boldsymbol{X}^*, \quad \boldsymbol{S}^0 = \boldsymbol{S}^*, \quad \lambda_i^0 := \beta_i \bar{d}_i - \sum_{j\in J} Y_{ij}^*, \quad \forall i \in [I].$$

- **Step 3: Compute the location design and capacity initialization**. Execute the iteration process. In each iteration n, we use the online gradient descent algorithm to compute a near-optimal approximation for $\boldsymbol{S}^{n*}$.
  - *Step 3.1.* For $k = 1, 2, \ldots, K$, do the following:
    - Solve the following primal problem given the demand scenario $\hat{\boldsymbol{d}}(k)$ and the Lagrangian dual multiplier $\boldsymbol{\lambda}^n$:

$$\min \quad \sum_{i\in[I]} \left[\sum_{j\in[J]} (\eta c_{ij} - \lambda_i^n) Y_{ij}(k) + \bar{p}_i W_i(k) \right],$$

$$\text{s.t.} \quad \sum_{j\in \text{Cov}_i} Y_{ij}(k) + W_i(k) \geq \hat{d}_i(k), \quad \forall i \in [I],$$

$$\sum_{i\in \text{Dem}_j} Y_{ij}(k) \leq S_j^n(k-1), \quad \forall j \in [J],$$

$$W_j(k) \geq 0, \quad \forall j \in [J],$$

$$Y_{ij}(k) \geq 0, \quad \forall i \in [I], j \in [J],$$

    - Solve the following dual problem:

$$\max \quad \sum_{i\in[I]} \hat{d}_i(k) u_i(k) + \sum_{j\in[J]} S_j^n(k-1) v_j(k),$$

$$\text{s.t.} \quad b_{ij}\big(u_i(k) + v_j(k)\big) \leq \eta c_{ij} - \lambda_i^n, \quad \forall i \in [I], j \in [J]$$

$$u_i(k) \leq \bar{p}_i, \quad \forall i \in [I],$$

$$u_i(k) \geq 0, \quad \forall i \in [I],$$

$$v_j(k) \leq 0, \quad \forall j \in [J],$$

    where $b_{ij} = 1$ if $c_{ij} \leq T_{\max}$, otherwise, $b_{ij} = 0$.
    - Update the capacity. Denote the step size $\gamma(k) := \frac{1}{\sqrt{k}}$ and step direction

$$\nabla_{S_j^n(k-1)} f(\cdot) := \mathbf{1}_{S_j^n(k-1)=0} \cdot f_j + \bar{a}_j + v_j(k),$$

    where $\mathbf{1}(\cdot)$ is the indicator function. $v_j(t)$ denotes the optimal solution to the dual problem that corresponds to the capacity constraint, and thus, its value depends on $\boldsymbol{S}^n(k-1)$. Here, $\mathbf{1}_{S_j^n(k-1)=0} \cdot f_j + \bar{a}_j$ denotes the cost of increasing capacity, while $v_j(k)$ is the profit as capacity increases. Therefore, if $\nabla_{S_j^n(k-1)} f(\cdot) \leq 0$, the planner tends to increase the capacity; otherwise, the capacity should be decreased to reduce cost. Thus, we define the gradient as follows:

$$S_j^n(k) := \max\left\{ S_j^n(k-1) - \gamma(k) \nabla_{S_j^n(k-1)} f(\cdot), 0 \right\}.$$

  - *Step 3.2.* Compute the average capacity and expected allocation quantity on each flow over K scenarios:

$$\bar{\boldsymbol{S}}^n = \frac{\sum_{k=1}^K \boldsymbol{S}^n(k-1)}{K}, \quad \bar{Y}_{ij}^n := \frac{\sum_{k=1}^K Y_{ij}^n(k)}{K}.$$

    where $Y_{ij}^n(k)$ denotes the optimal solution to the primal problem in scenario k with fixed $\boldsymbol{\lambda}^n$.
- **Step 4: Dual multiplier update**. Update the dual multiplier $\boldsymbol{\lambda}^{n+1}$ as follows:

$$\lambda_i^{n+1} := \lambda_i^n + \frac{1}{\sqrt{n}} \left(\beta_i \frac{\sum_{k=1}^K d_{jt}}{K} - \sum_{j\in J} Y_{ij}^n \right).$$

  where $\frac{1}{\sqrt{n}}$ represents the step size.
- **Step 5: Iterate until the algorithm terminates**. Define a predetermined tolerance threshold ϵ and terminate the above process when $\max_{i\in I} \left\{ \lambda_i^{n+1} - \lambda_i^n \right\} \leq \epsilon$. Then, the optimal capacity $\boldsymbol{S}^* = \bar{\boldsymbol{S}}^n$, the optimal location design $\boldsymbol{X}^* = \bar{\boldsymbol{X}}^n$, and the corresponding initial assignment policy $\boldsymbol{Y}^* = \bar{\boldsymbol{Y}}^n$ constitute the desired profile. Otherwise, let $n = n + 1$ and go back to Step 3.

In Step 3 of Algorithm 1, we employ an online gradient descent algorithm to achieve a near-optimal approximation of $\boldsymbol{S}^{n*}$. Specifically, we aim to minimize the average regret from using $\left\{\boldsymbol{S}^n(k)\right\}_{k=1}^K$ over K scenarios, defined as

$$\text{Regret(K)} := \frac{1}{\text{K}} \left[\sum_{\text{k}=1}^{\text{K}} \text{f}_\text{k}^\text{n}(\boldsymbol{\lambda}^\text{n}, \boldsymbol{X}^\text{n}, \boldsymbol{S}^\text{n}, \hat{\boldsymbol{d}}(\text{k})) - \sum_{\text{k}=1}^{\text{K}} \text{f}_\text{k}^\text{n}(\boldsymbol{\lambda}^{\text{n}*}, \boldsymbol{X}^{\text{n}*}, \boldsymbol{S}^{\text{n}*}, \hat{\boldsymbol{d}}(\text{k})) \right]. \tag{11}$$

Theorem 4.1 is proposed to guarantee the performance of the online gradient descent algorithm. That is, the results obtained by the

online gradient descent algorithm are a near-optimal solution of $\boldsymbol{X}^{n*}$.

Theorem 4.1. *The average regret of the online gradient descent algorithm satisfies the following nonasymptotic bound:*

$$\text{Regret(K)} \leq \mathcal{O}(\frac{1}{\sqrt{\text{K}}}). \tag{12}$$

Proof. The detailed proof is displayed in Appendix A.1. □

Theorem 4.1 shows that as K tends to infinity, the gap between our method and the optimal solution tends to be 0. This means our method can obtain the optimal solution when $K \to \infty$. Furthermore, our method has an enormous advantage in that the computational complexity increases linearly with increasing K. Therefore, the computational difficulty of our method only depends on the complexity of the subprimal and subdual problems. However, the traditional method, which can obtain the optimal solutions, needs to address all K samples simultaneously. It is intractable when $K \to \infty$, since the computational complexity increases exponentially with the increase of K.

4.3. Phase II (Operational Phase): Dynamic capacity planning

Given the location design X_j and capacity initialization $S_j(1)$ obtained from subsection 4.2, we address a dynamic capacity planning problem to fulfill the requirements during the operational phase of each time period. In each time period t, we need to decide the capacity increment $\Delta S_j(t)$, the allocation schedule $Y_{ij}(t)$ and the corresponding unmet demand $W_i(t)$.

In this subsection, we propose two allocation policies, which can be implemented in different requirements:

- **Dynamic allocation (DA) policy with a single objective.** This policy applies in the scenario where the planner focuses on the minimization of the total cost.
- **Adaptive dynamic allocation (ADA) policy with multiple objectives.** This policy focuses on the case in which the planner has multiple predetermined targets and aims to achieve all these targets within a long time period.

4.3.1. Dynamic allocation policy with a single objective

This policy is an intuitive allocation policy that solves the following submodel period by period. For each $t, t \in [T]$,

$$[\text{Sub1(t)}] \quad \min \quad \sum_{j\in[J]} a_{jt}\Delta S_j(t) + \eta \sum_{i\in[I]}\sum_{j\in[J]} c_{ij}Y_{ij}(t) + \sum_{i\in[I]} p_{it}W_i(t), \tag{13a}$$

$$\text{s.t.} \quad \sum_{j\in \text{Cov}_i} Y_{ij}(t) \geq \beta_i d_i(t), \quad \forall i \in [I], \tag{13b}$$

$$\sum_{j\in \text{Cov}_i} Y_{ij}(t) + W_i(t) \geq d_i(t), \quad \forall i \in [I], \tag{13c}$$

$$\sum_{i\in \text{Dem}_j} Y_{ij}(t) \leq \Delta S_j(t) + S_j(t-1), \quad \forall j \in [J], \tag{13d}$$

$$\Delta S_j(t) \leq MX_j, \quad \forall j \in [J], \tag{13e}$$

$$\Delta S_j(t), W_j(t) \geq 0, \quad \forall j \in [J], \tag{13f}$$

$$Y_{ij}(t) \geq 0, \quad \forall i \in [I], j \in [J]. \tag{13g}$$

This policy focuses on the minimization of total cost.

4.3.2. Adaptive dynamic allocation policy

In practice, planners may have some predetermined targets before making decisions. For example, in humanitarian logistics, they aim to reduce the quantity of the unmet demand to zero. Therefore, in this subsection, we adopt an adaptive dynamic allocation policy, which can achieve all these targets if they are attainable and can obtain a point that is closest to the unattainable target.

To better meet the requirements of this problem compared with the dynamic policy in subsection 4.3.1, we consider the following three objectives: varying capacity construction cost, transportation cost, and penalty cost for unmet demand. In addition, other objectives can also be involved, which has no influence on the following analysis. The three objectives are given as follows:

$$g_1(\cdot, \boldsymbol{d}(t)) = \sum_{j\in[J]} a_{jt}\Delta S_j(t),$$

$$g_2(\cdot, \boldsymbol{d}(t)) = \eta \sum_{i\in[I]}\sum_{j\in[J]} c_{ij}Y_{ij}(t),$$

$$g_3(\cdot, \boldsymbol{d}(t)) = \sum_{i\in[I]} p_{it}W_i(t).$$

In a long period of time, the decision-maker aims to address the following multiobjective problem:

$$[\text{AM0}] \quad \min \quad \left\{\frac{1}{T}\sum_{t=1}^{T} g_1(\cdot, \boldsymbol{d}(t)), \quad \frac{1}{T}\sum_{t=1}^{T} g_2(\cdot, \boldsymbol{d}(t)), \quad \frac{1}{T}\sum_{t=1}^{T} g_3(\cdot, \boldsymbol{d}(t))\right\}, \tag{14a}$$

$$\text{s.t.} \quad \sum_{j\in \text{Cov}_i} Y_{ij}(t) \geq \beta_i d_i(t), \quad \forall i \in [I], t \in [T], \tag{14b}$$

$$\sum_{j\in \text{Cov}_i} Y_{ij}(t) + W_i(t) \geq d_i(t), \quad \forall i \in [I], t \in [T], \tag{14c}$$

$$\sum_{i\in \text{Dem}_j} Y_{ij}(t) \leq \Delta S_j(t) + S_j(t-1), \quad \forall j \in [J], t \in [T], \tag{14d}$$

$$\Delta S_j(t) \leq MX_j, \quad \forall j \in [J], t \in [T], \tag{14e}$$

$$\Delta S_j(t), W_j(t) \geq 0, \quad \forall j \in [J], t \in [T], \tag{14f}$$

$$Y_{ij}(t) \geq 0, \quad \forall i \in [I], j \in [J], t \in [T]. \tag{14g}$$

The function $g_k(\cdot, \boldsymbol{d})$ denotes the kth objective function under scenario $\boldsymbol{d}$. In problem [AM0], each decision is made at period t using only the historical information available up to period t, i.e.,

$$\{\Delta \boldsymbol{S}(s), \boldsymbol{Y}(s), \boldsymbol{W}(s), \boldsymbol{d}(s)\}_{s=1}^{t-1} \cup \{\boldsymbol{d}(t)\},$$

while future information such as $\{\boldsymbol{d}(t+1), \cdots, \boldsymbol{d}(T)\}$ is unknown.

Next, we define the predetermined multiobjective target. Based on the solution of Phase I, we define the multiobjective targets $\boldsymbol{\tau} = \{\tau_1, \tau_2, \tau_3\}$, where $\tau_1 = 0$, $\tau_2 = \eta \sum_{i\in[I]}\sum_{j\in[J]} c_{ij}Y^*_{ij}$, $\tau_3 = 0$, and $\boldsymbol{Y}^*$ denotes the achieved assignment solution of Phase I. After obtaining the initial location and capacity decisions in Phase I, we further explain the values of three targets in Phase II as follows: (1) minimize the total varying capacity expansion cost; (2) ensure that the transportation cost is near the predetermined value in Phase I; and (3) try to decrease the total penalty cost to zero.

Let $\alpha_k(\boldsymbol{d})$ be the *debt* of objective k under scenario $\boldsymbol{d}$; i.e., the difference between target τ_k and $g_k(\cdot, \boldsymbol{d})$, $\alpha_k(\boldsymbol{d}) := g_k(\cdot, \boldsymbol{d}) - \tau_k$. In

the beginning of each period $t+1$, the average *debt* of objective k from periods 1 to t is recorded as $w_k(t+1)$; i.e.,

$$w_k(t+1) = \frac{1}{t}\sum_{s=1}^{t}\alpha_k(s). \tag{15}$$

Essentially, w_k is positively correlated with the weight of objective k. If the required target is not achieved, where $w_k(t+1) > 0$, we need to give higher priorities to objective k. Otherwise, for those $w_k(t+1) \le 0$, their corresponding objectives have already been achieved, and no additional attention is necessary. Altogether, we use the vector $w_k^+(t) = \max\{0, w_k(t)\}$ to quantify the gap between target τ_k and the current solution $g_k(\cdot, \boldsymbol{d}(t))$ at period t, which suggests the priority associated with each objective function. Next, we introduce our adaptive dynamic allocation policy.

Algorithm 2. Adaptive dynamic allocation policy for capacity planning.

- **Input**: Demand $\{\boldsymbol{d}(1), \boldsymbol{d}(2), \cdots, \boldsymbol{d}(T)\}$.
- **Output**: Adjusted capacity $\tilde{\boldsymbol{S}}^*$.
- **Step 1**: Initialization. Set $t = 1$, initial weight $\boldsymbol{w}(1) = \{1, 1, 1\}$.
- **Step 2**: Solve the subproblem.

$$[\text{Sub2(t)}] \quad \min \quad \sum_{k=1}^{3} w_k^+(t)\cdot g_k(\cdot, \boldsymbol{d}(t)), \tag{16a}$$

$$\text{s.t.} \quad \sum_{j\in \text{Cov}_i} Y_{ij}(t) \ge \beta_i d_i(t), \quad \forall i \in [I], \tag{16b}$$

$$\sum_{j\in \text{Cov}_i} Y_{ij}(t) + W_i(t) \ge d_i(t), \quad \forall i \in [I], \tag{16c}$$

$$\sum_{i\in \text{Dem}_j} Y_{ij}(t) \le \Delta S_j(t) + S_j(t-1), \quad \forall j \in [J], \tag{16d}$$

$$\Delta S_j(t) \le M X_j, \quad \forall j \in [J], \tag{16e}$$

$$\Delta S_j(t), W_j(t) \ge 0, \quad \forall j \in [J], \tag{16f}$$

$$Y_{ij}(t) \ge 0, \quad \forall i \in [I], j \in [J]. \tag{16g}$$

- Step 3: Update weights. For $k = 1, 2, 3$, we update the weights as follows:

$$w_k^+(t+1) = \max\left\{\frac{(t-1)w_k(t) + g_k(\cdot, \boldsymbol{d}(t)) - \tau_k}{t}, 0\right\}, \tag{17}$$

Update $t = t+1$ and return to Step 2 if $t < T$; otherwise, adjust the final $\tilde{S}_j^*$ by the incumbent number ΔS_j; thus, export $\tilde{\boldsymbol{S}}^* = \tilde{\boldsymbol{S}}^* + \Delta \boldsymbol{S}(T)$.

As a minimization problem, $g_k(\cdot, \boldsymbol{d}(t))$ converges to τ_k from the top during the iterations; therefore, $\alpha_k(\boldsymbol{d}) \ge 0$ at the initial stages. Definition (17) indicates that the objectives that deviate much from the corresponding target should receive more weight in the next period.

Let g_k^* be the performance of objective k with the target-based optimal solution to an expected single-period problem; when objective 3 is taken as an example, $g_3^* = \mathbb{E}_{[D]}\left[\sum_{i\in[I]} p_{it} W_i(\boldsymbol{d})\right]$. Moreover, let $w_k^* = \tau_k - g_k^*$ represent the *debt* vector of the single-period problem (g_k^*) with respect to target k (τ_k). Recall the theorem proposed by Lyu et al. (2019b), which gives the theoretical performance guarantee of the proposed ADA policy $\boldsymbol{w}^+(T+1)$ and the expected single-period model $(\boldsymbol{w}^*)^+$.

Theorem 4.2. *(Lyu et al., 2019b) Consider the multiperiod, multi-objective dynamic capacity planning problem* [AM0]. *Weight vector* $\boldsymbol{w}(t)$ *under the ADA policy converges to the optimal weight vector* $\boldsymbol{w}^*$. *Specifically, it satisfies the following:*

$$\mathbb{E}\left[||\boldsymbol{w}^+(T+1)||_2^2\right] - \mathbb{E}\left[||(\boldsymbol{w}^*)^+||_2^2\right] \le \mathcal{O}\left(\frac{1+\log T}{T}\right), \tag{18}$$

where the expectation in inequality (18) is taken over $\boldsymbol{d}_1, \boldsymbol{d}_2, \ldots, \boldsymbol{d}_T$, *and* $||\cdot||_2$ *is the Euclidean norm of a vector.*

Proof. For the details of the proof, we refer readers to Lyu et al. (2019b). □

We make the following three remarks about our policy. First, our policy can be used to examine the attainability of any predetermined targets. If the Euclidean norm of the vector $\boldsymbol{w}(T+1)$ would not converge to 0 as T increases by using the ADA policy, then the corresponding target cannot be attained by any other non-anticipative policies. Second, the ADA policy is indeed nonanticipatory since the average vector $\boldsymbol{w}(T+1)$ at period $(t+1)$ is calculated based on the debt from period 1 to t without observing future information. Third, the ADA policy does not require tracking another status of the system and can be easily applied to solve large-scale problems in real time.

5. Case study

In this section, we use a case study to verify the efficiency and effectiveness of the proposed approaches. Testing data are generated based on a case study related to the preparedness phase of testing facility location design under pandemic threats.

A laptop with an Intel Core 5 Duo 2.2 GB CPU and 4 GB of RAM and running Windows 10 is used to conduct all numerical experiments. We employ CPLEX 12.8 as the MILP, and the procedure terminates with a relative optimality tolerance 10^{-4}.

5.1. Instance generation

With respect to the time during COVID-19 exposure, we combine three sources of data as inputs to find the optimal locations of testing facilities and their corresponding capacity in Beijing, China. The first source is from the COVID-19 Data Repository (Dong, Du, & Gardner, 2020), which is attributed to *the Center for Systems Science and Engineering (CSSE) at Johns Hopkins University* from GitHub (https://github.com/CSSEGISandData/COVID-19). The database achieved a complete list of all sources related to COVID-19, which includes the time series data of a number of confirmed cases, deaths, and recovered cases. In this paper, we adopt the number of active cases in Beijing from January 21, 2020, to September 27, 2020 (250 days in total). Fig. 2 illustrates the critical trend of active COVID-19 cases, in which the peak value is 326, occurring on June 30, 2020.

The second source is demographic and economic data from the Chinese census bureau or business investigation. The total population of 333 citywide towns from Beijing based on the 5*th* national census in 2010 is summarized and is available from China National Knowledge Infrastructure (CNKI). The average housing price of districts in Beijing is derived from Anjuke Corporation and is used to evaluate fixed facilities construction cost.

The third source is the geographic data from Gaode web API. After the selection of demand sites and facility candidates, we obtain their corresponding longitudes and latitudes via Python 3.6 from *Gaode*. To better visualize the computational results, boundary data of the 16 districts of Beijing are also obtained in a similar manner. Fig. 3 illustrates the locations of candidate facilities (green triangles) and demand sites (black dots), where Fig. 3a depicts the

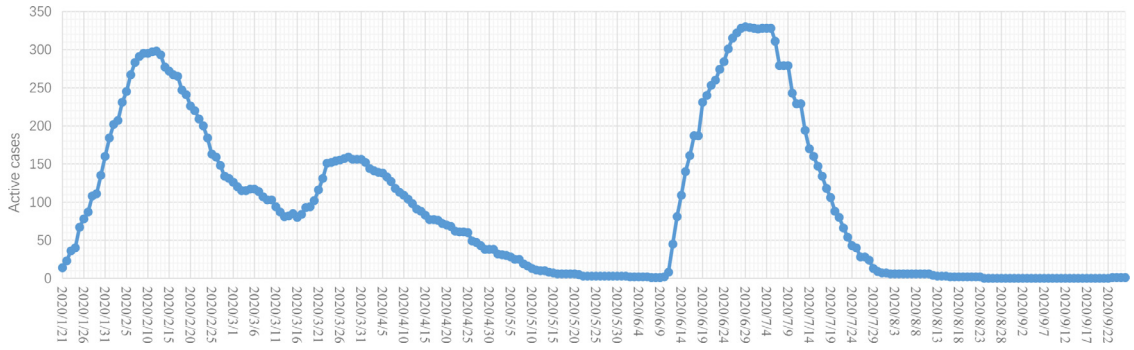

Fig. 2. Active COVID-19 cases in Beijing from January 21, 2020, to September 27, 2020.

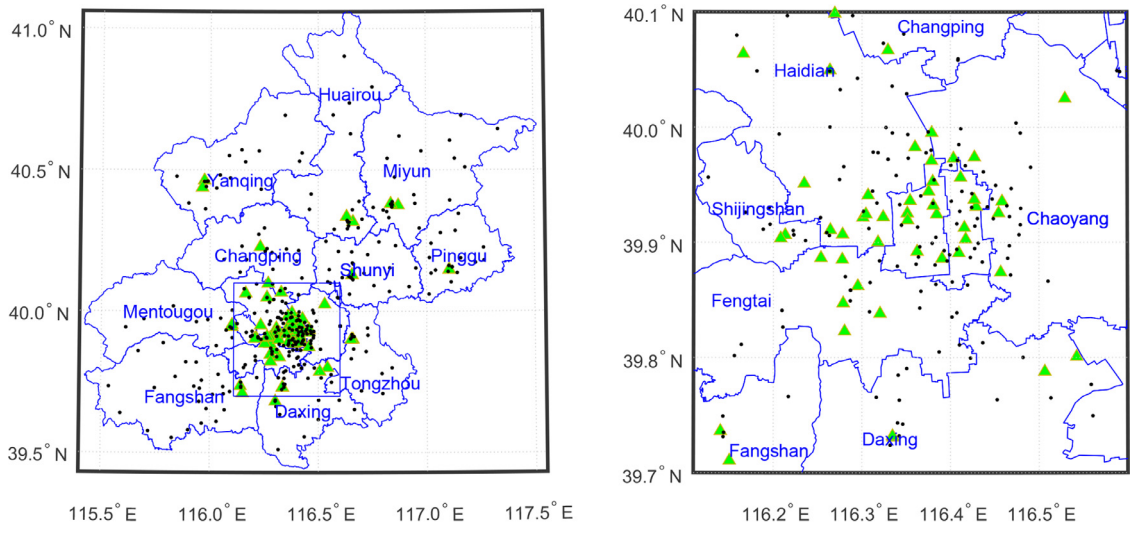

(a) Citywide (b) Downtown area

Fig. 3. Locations of demand sites and facility candidates.

distribution of critical nodes across the city, and Fig. 3b focuses on details in the downtown area.

The candidate facilities can be generally classified into four categories: 3A hospitals, regional hospitals, regional centers for disease control and prevention (CDCs), and commercial testing institutes. Interested readers can find details on facility candidates from Table D.8 of Appendix D. After gathering data from the above data sets, we summarize the input parameters as follows.

$[J]$	66 facility candidates including 3A or regional hospitals, regional CDCs and commercial testing institutes.
$[I]$	333 geographical centers of towns across from Beijing.
$[T]$	250 days from January 21, 2020, to September 27, 2020.
f_j	see Table D.8 of Appendix D.
a_{jt}	see Table D.8 of Appendix D.
c_{ij}	distance between facility candidate j and demand site i (km).
η	set as 0.001.
p_{it}	set as 6, $\forall i \in [I]$, $t \in [T]$.
d_{it}	assume that the number of active cases in period t is N_t, $t \in [T]$, $N_{\max} = \max_{t\in[T]} N_t$, then $d_{it} = \frac{\text{population of town } i * N_t}{N_{\max}}$.

5.2. Performance validation of the OCO-based LR

In Phase I, problem [P2] associated with uncertain demand could be solved by SAA and the OCO-based LR approach. We conduct several numerical experiments to compare the asymptotic consistency and computational efficiency. SAA is solved by CPLEX with a time limit of 3600 seconds. Note that there are many methods to solve the SAA formulation, such as Benders decomposition. These algorithms do not reduce the complexity of the problem. Therefore, even if these algorithms can improve computational efficiency, the improvement will not be too large. Therefore, for convenience, we choose a commercial solver, i.e., CPLEX, as a benchmark. The number of input demands K is increased from 100 to 5,000; let $\bar{d}_i$ be the expected value observed demand of town i from January 21, to September 27, 2020. d_{ik} is uniformly generated from $U[0.9\bar{d}_i, 1.1\bar{d}_i]$, $\forall k \in \{1, \cdots, K\}$. We set $J \in \{10, 20, 30, 40, 50, 66\}$ and $I \in \{50, 100, 150, 200, 250, 333\}$, which are randomly selected from the 66 facility candidates and 333 town centers. Each instance is run 10 times, and we summarize the average performance.

Table 2 indicates that CPLEX could not obtain an optimal solution for the instances when $K \geq 200$ within 3600 seconds, while OCO-based LR can obtain a near-optimal solution with a linearly increasing computational time (see Fig. 4). Generally, scenario-based approaches are not applicable to the decision problems that we work on. We will have a very large number of scenarios, which is time-consuming to compute the average value or expectation. Interestingly, our OCO-based LR can solve the instance with 66 facility candidates and 333 demand sites with 5000 scenarios within an hour. The last column represents the objective gap between CPLEX and OCO-based LR. For instances with few scenarios, say $K = 100$, OCO-based LR obtains a near-optimal solution (no more than 0.3% higher than the optimal values) in no more than one

Table 2
Comparisons between CPLEX and OCO-based LR for the first-phase problem.

Para			CPLEX		OCO-based LR		Comparisons	
J	I	K	Time1	Obj1	Time2	Obj2	Gap-Time (%)	Gap-Obj (%)
10	50	100	1623.2	4280.6	3.1	4291.6	99.8	-0.3
10	50	200	3600.0	4392.2	6.3	4314.2	99.8	1.8
10	50	500	3600.0	5151.9	14.9	4321.3	99.6	16.1
10	50	1000	3600.0	–	39.5	4321.5	98.9	–
10	50	5000	3600.0	–	228.4	4321.2	93.7	–
20	100	100	1589.9	8133.7	9.6	8149.1	99.4	-0.2
20	100	200	3600.0	8362.4	19.0	8192.1	99.5	2.0
20	100	500	3600.0	9882.1	48.1	8205.6	98.7	17.0
20	100	1000	3600.0	–	118.6	8205.9	96.7	–
20	100	5000	3600.0	–	691.0	8205.3	80.8	–
30	150	100	1619.7	11205.9	16.6	11214.7	99.0	-0.1
30	150	200	3600.0	11560.0	34.4	11273.8	99.0	2.5
30	150	500	3600.0	13964.6	83.8	11292.4	97.7	19.1
30	150	1000	3600.0	–	196.8	11292.9	94.5	–
30	150	5000	3600.0	–	1197.8	11292.2	66.7	–
40	200	100	1719.2	13772.7	21.9	13790.3	98.7	-0.1
40	200	200	3600.0	14341.7	49.2	13863.0	98.6	3.3
40	200	500	3600.0	17720.8	118.8	13885.9	96.7	21.6
40	200	1000	3600.0	–	265.0	13886.4	92.6	–
40	200	5000	3600.0	–	1642.8	13885.5	54.4	–
50	250	100	1743.2	16306.3	27.6	16330.3	98.4	-0.1
50	250	200	3600.0	17265.5	60.8	16416.3	98.3	4.9
50	250	500	3600.0	21315.2	146.6	16443.4	95.9	22.9
50	250	1000	3600.0	–	316.7	16444.0	91.2	–
50	250	5000	3600.0	–	1905.7	16443.0	47.1	–
66	333	100	1982.9	20529.2	39.0	20538.9	98.0	0.0
66	333	200	3600.0	21871.7	80.4	20647.1	97.8	5.6
66	333	500	3600.0	27132.3	205.1	20681.1	94.3	23.8
66	333	1000	3600.0	–	424.9	20681.9	88.2	–
66	333	5000	3600.0	–	2581.2	20680.6	28.3	–

Note: "–" means no solution can be searched in 3600 seconds. Time1 and Time2 represent the CPU time of CPLEX and OCO-based LR, respectively; Obj1 and Obj2 indicate the objective value of CPLEX and OCO-based LR, respectively. Gap-Time $= \frac{\text{Time1-Time2}}{\text{Time1}} \times 100\%$ and Gap-Obj $= \frac{\text{Obj1-Obj2}}{\text{Obj1}} \times 100\%$.

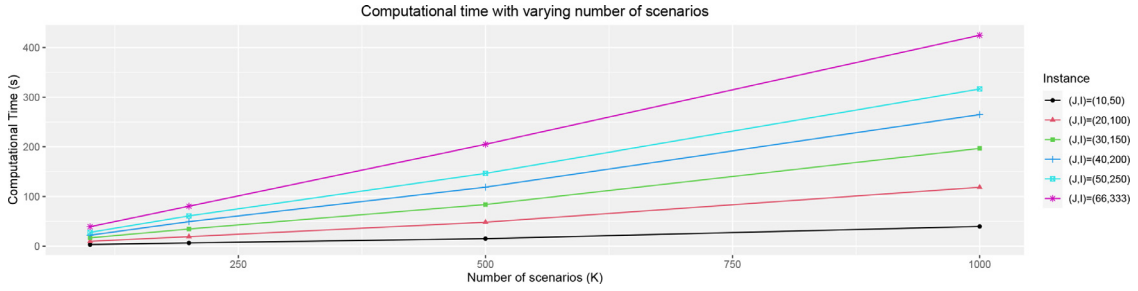

Fig. 4. Computational time of OCO-based LR with varying numbers of scenarios (K).

minute, while the computational time of CPLEX is more than half an hour. The advantage of OCO-based LR is even significant when K increases. For example, when $K = 1000$, CPLEX could not obtain any feasible solution within 3600 seconds, and LR converges in no more than 10 minutes. The results of numerical experiments show the superiority and effectiveness of our algorithm for solving the first-phase problem.

Figure 5 illustrates the convergence performance of OCO-based LR based on the empirical data defined in Section 5.1. Within 3600 seconds, CPLEX obtains an optimal solution with a lower bound of 19,965.2 and an upper bound of 23,798.5. LR converges to the near-optimal 20,676.3 in 107 seconds through 26 iterations.

5.3. Performance validation of the two-phase framework

To validate the effectiveness of our proposed two-phase framework, we adopt three benchmark policies: DM-F, DM-P, and DA. Although many methods can be used to solve classic settings, such as dynamic programming and Markov decision processes, they are difficult to implement to solve the settings under pandemics, as introduced in Section 1. Therefore, we select our own benchmarks. Specifically, Policy 1 (DM-F) can obtain the ideal optimal solution since it solves the settings in which all future information is known in advance. If our methods can achieve a solution very close to the ideal optimal solution, then we can validate that our method is effective. A total of five methods are implemented to solve the instance introduced above. Table 3 summarizes the inputs and methods that have been employed in each policy, and detailed descriptions of these approaches are listed below.

- **Policy 1. Deterministic model with full information (DM-F).** We solve the multiperiod deterministic model [P1] with perfect knowledge of future demand. That is, it is assumed that all future information is known at the beginning of the first phase. However, it is impossible to obtain such full information in practice. Thus, this policy is treated only as a comparison of others, which provides the optimal solution in an ideal setting.
- **Policy 2. Deterministic model with predicted information (DM-P).** We first apply a forecasting model to predict the future

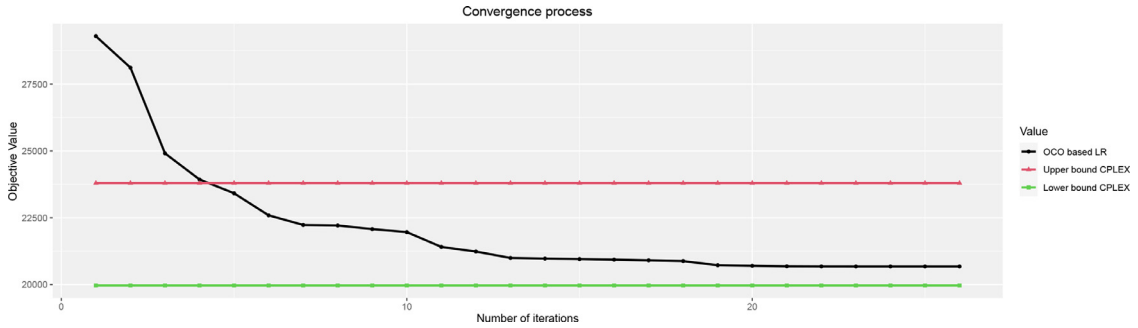

Fig. 5. Convergence of OCO-based LR algorithm (instance with 66 facility candidates, 333 demand cites with $K = 250$ scenarios).

Table 3
Summary of the results for five policies.

Policy	First-Phase		**Second-Phase: period** t	
	Input	Method	Input	Method
DM-F	Actual demand d_{it}	Solve [P1] by CPLEX	–-	–-
DM-P	Predicted demand $\hat{d}_{it}$	Solve [P1] by CPLEX	–-	–-
DA	–-	–-	d_{it}, $X_j(t-1)$, $S_j(t-1)$	Solve single-period problem by CPLEX
LR-DA	Predicted demand $\hat{d}_{it}$	OCO-based LR	d_{it}, $S_j(t-1)$	Dynamic allocation policy
LR-ADA	Predicted demand $\hat{d}_{it}$	OCO-based LR	d_{it}, $S_j(t-1)$	ADA policy

Table 4
Comparisons of computational time and optimal solution of the five policies .

Metric	DM-F	DM-P	DA	LR-DA	LR-ADA
CPU time (s)	2592	2354	496	769	775
Fixed cost	10,877	12,022	7591	16,791	16,791
Varying construction cost	575,880	1,159,160	555,472	621,708	621,810
Transportation cost	353,817	698,763	426,600	333,656	332,753
Penalty cost	0	66	0	0	0
Total cost	940,574	1,870,010	989,663	972,155	971,354
Total amount of facilities built	24	26	18	34	34
Gap_π (%)	0.0	98.8	5.2	3.4	3.3

demand and then solve the multiperiod deterministic model [P1] with predicted demand. In this paper, we generate the predicted demand randomly; i.e., the predicted value $\hat{d}_i(t)$ is located uniformly in the range of $[0.95d_t(t), 1.05d_i(t)]$.

- **Policy 3. Dynamic allocation policy (DA)**. We solve the single-period problems iteratively T times, and each problem corresponds to sequentially realized demand $d_i(t)$. In addition, the location and capacity strategies obtained at the current time period are set as the inputs of the next time period.
- **Policy 4. Lagrangian relaxation-based dynamic policy (LR-DA)**. We apply our two-phase approach to solve the problem. In the first phase, the LR algorithm introduced in Section 4.2 is introduced, and the second phase program is approached by the dynamic allocation policy in Section 4.3.1.
- **Policy 5. Lagrangian relaxation-based adaptive dynamic allocation policy (LR-ADA).** The difference between Policies 4 and 5 is that we employ the ADA policy (see Section 4.3.2) in the second phase of Policy 4.

Table 4 summarizes the results of the five policies. The results show that the last three policies have an obvious advantage in computational time. The DA policy takes less time to solve than our two policies since our policies have one more location design and capacity initialization process. In actuality, the computational time of our two policies is acceptable in practice. For the total cost, we define a metric to measure the distance from the last four policies to the optimal one as follows:

$$\text{Gap}_\pi = \frac{TC_\pi - TC_{\text{DM-F}}}{TC_{\text{DM-F}}} \times 100\%, \quad \forall \pi \in \{\text{DM-P, DA, LR-DA, LR-ADA}\}$$

The DM-P policy achieves a gap of 98.8%, which means that a very small prediction error leads to enormous cost consumption. Therefore, the DM-P policy is not suitable to solve this problem. Our two policies can obtain gaps of 3.4% and 3.3%, which are smaller than the gap of 5.2% obtained by the DA policy. In summary, our two policies obtain the solution with the minimum distance from the ideal optimal solution in a very short time. Specifically, the LR-ADA policy achieves the solution with the minimum total cost.

Figure 6 shows the results of location decisions in Phase I, and the background color represents the total population (which is proportional to demand). Note that Policies LR-DA and LR-ADA have the same results, which are plotted in Fig. 6(d). We can observe that our two policies build 34 facilities, more than the other three policies. This is because our policies consider future demand inflation when making location decisions by using a sample set with K scenarios. This can help reduce the varying construction and transportation cost in the future time period. The DA policy only builds 18 facilities during the first time period. However, its construction and transportation widely vary cost.

5.4. Real-time performance

Next, we focus on real-time performance. We define the average cost until time period t, i.e.,

$$\text{cost}_t = \frac{1}{t}\sum_{s=1}^{t} \text{objective value}_s.$$

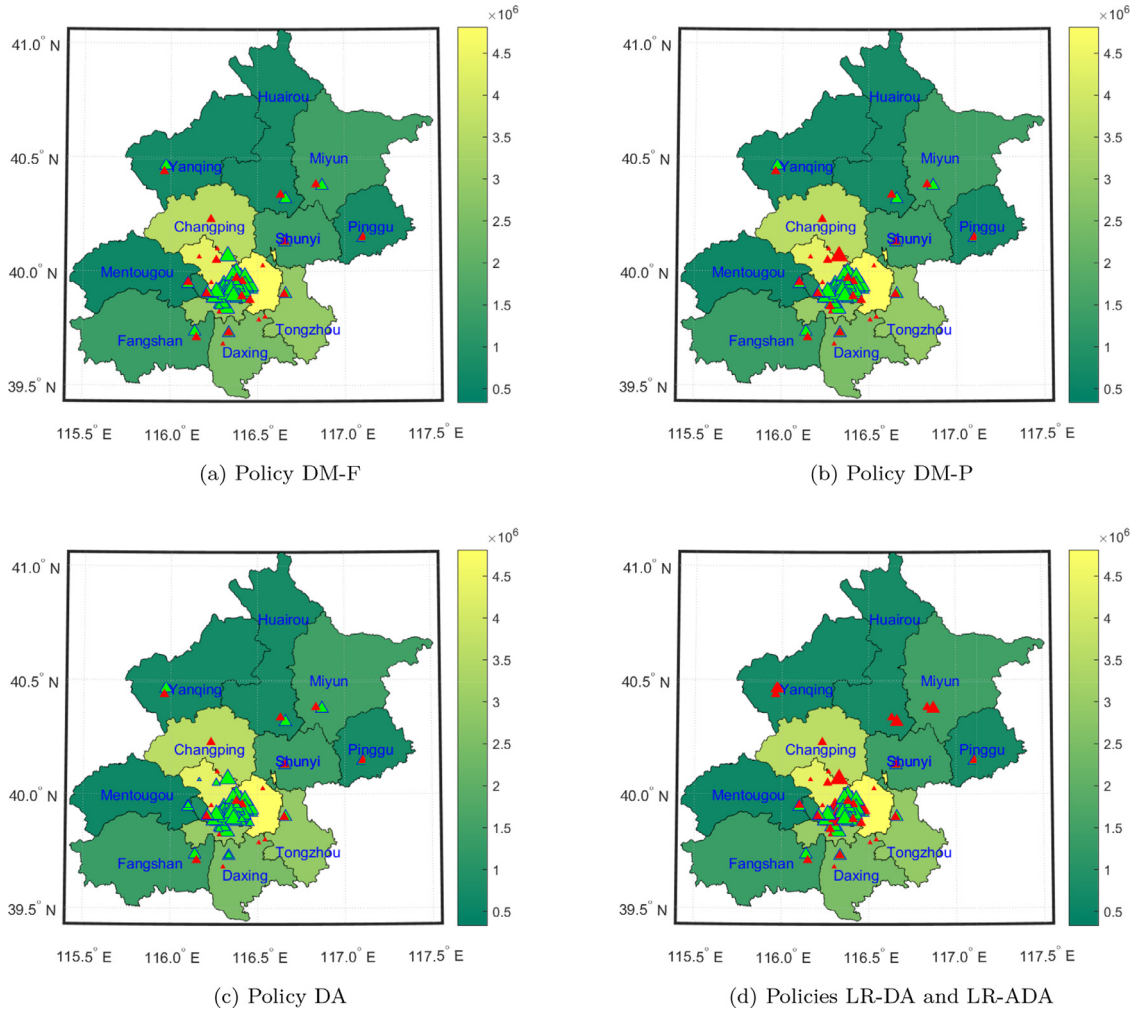

(a) Policy DM-F

(b) Policy DM-P

(c) Policy DA

(d) Policies LR-DA and LR-ADA

Fig. 6. Optimal location strategies.

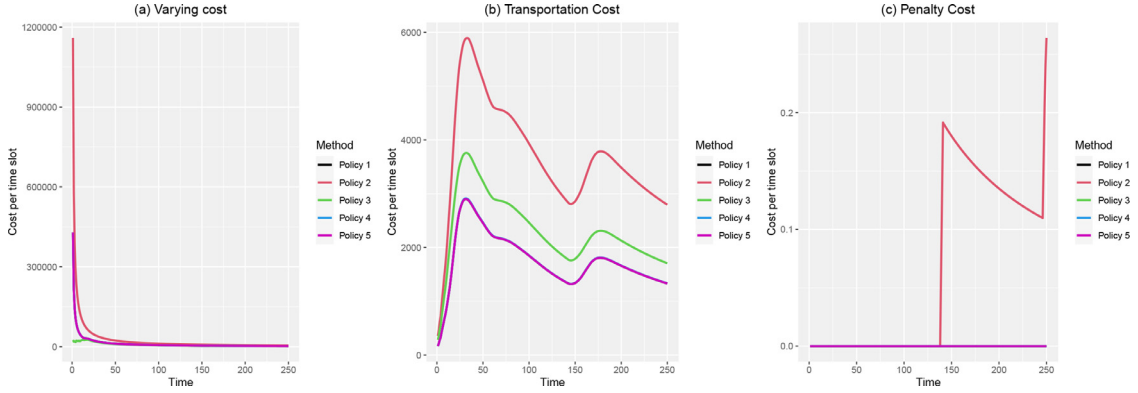

Fig. 7. Average cost performance along the time dimension.

Fig. 7 reports the results along the time dimension. Obviously, the DM-P policy incurs most of the cost of the capacity expansion due to an imprecise prediction. The two-phase LR-DA and LR-ADA policies perform well on the metric of varying cost. The transportation cost has a trend similar to the demand trend for all of the policies. Specifically, the LR-DA and LR-ADA policies perform the best, DA takes the second place, and the DM-P policy is in the last place. As unmet demand is not expected, the unit penalty cost p_{it} is assumed to be relatively large. Therefore, the penalty cost of all policies is almost zero, except the DM-P policy, which also has little penalty cost.

We define the regret of total cost (TC) as follows:

$$Regret^{\pi}(t) = \sum_{s=1}^{t} \left(TC_s^{\pi} - TC_t^{\text{DM-F}} \right), \quad \forall \pi \in \{\text{DM-P, DA, LR-DA, LR-ADA}\}. \tag{19}$$

Figure 8 displays the results of regret along the time horizon. First, looking at Fig. 8(a), we can observe that the DM-P policy achieves a very large regret, which means it performs the worst among the four policies. For the DA policy, although it performs the best during the first 100 days because of the relatively small

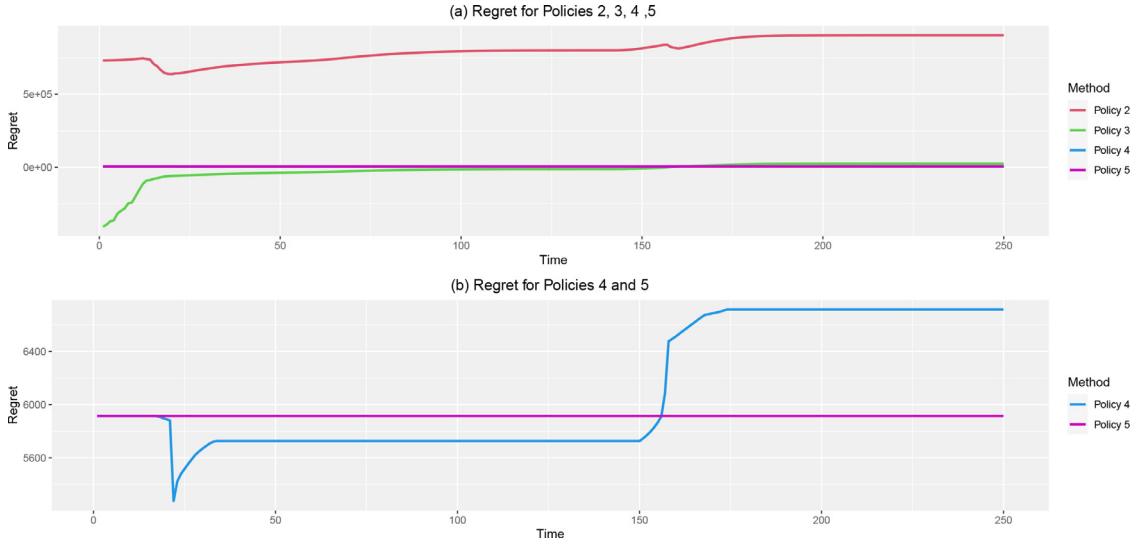

Fig. 8. Regret of total cost along the time dimension.

fixed cost, it obtains a larger regret than our two policies because of the increment of varying construction and transportation cost. For Fig. 8(b), it is obvious that the regret of the LR-DA policy fluctuates over time, while the LR-ADP policy converges gradually and stabilizes. Finally, compared with LR-DA, LR-ADP obtains a smaller regret, which highlights its superiority.

6. Conclusions and discussions

In this paper, we propose a two-phase framework to optimize location and capacity design strategies during pandemics. Decisions pre- and postpandemic are merged in a sequential framework. In the first phase, strategic decisions, such as facility location and capacity initialization, are determined with predicted demand. Instead of solving scenario-based SP by SAA, we creatively develop an OCO approach with Lagrangian multipliers and prove its asymptotic consistency. In the second phase, two allocation policies, DA and ADA, are designed to adjust capacities with respect to fluctuating demands. Compared with the other three traditional policies, our two-phase framework shows great benefits from the perspectives of computational time and performance validation based on a real case study of the COVID-19 situation in Beijing.

Several observations can be summarized from the numerical results.

- The OCO-based LR method in Phase I overcomes the “curse of dimensionality“ by SAA, providing a near-optimal and convergent solution in polynomial time, which dramatically increases computational efficacy.
- The two-phase framework prefers relatively robust location solutions (building more facilities at the beginning) and performs much better in terms of transportation and penalty costs while facing real-time demand volatility.
- For the two proposed two-phase solution approaches, LR-ADA admits a convergent and stable regret compared with LR-DA, as the asymptotic consistency of ADA has been theoretically proven.

We present several limitations that could be further explored in future research. First, although capacity expansion and preventing closure of any constructed facilities are common assumptions in a dynamic facility location and capacity planning problem (Charles et al., 2016; Jabbarzadeh et al., 2014; Shulman, 1991; Vatsa & Jayaswal, 2021; Yu & Shen, 2020), adding capacity is not always commensurate with the background of pandemics. For example, for large-scale infectious diseases (such as COVID-19) that may have multiple waves and reinfections (Arruda, Pastore, Dias, & Das, 2021), capacity initialization can be very costly based on early data. Incorporating new decisions, such as reducing or relocating testing facilities, is a beneficial way to reduce the total operational cost during the entire planning horizon. Second, there are many ways to formulate similar problems that belong to the scope of sequential decision-making with uncertainty (Powell, 2016; 2019a; 2019b); indeed, sometimes simpler formulations can be discovered. For example, the MDP formulation and ADP algorithm are possible approaches to solve the proposed problem, and we leave consideration of the MDP-based approach to future research. Finally, official datasets of an epidemic have been criticized for their poor reliability in terms of underestimation (Dyer, 2021) and statistical tests (Silva & Figueiredo Filho, 2021), which may lead to unrealistic demand scenarios in the model. Thus, it is necessary to improve the reliability of input data before optimization instead of directly implementing open-access datasets.

Acknowledgment

This research is partly supported by the National Natural Science Foundation of China (grant number 72101021), the fellowship of China Postdoctoral Science Foundation (grant number 2021M690009), and the Fundamental Research Funds for the Central Universities (grant number 2021RC202).

Appendix A. Proofs

A1. Proof of Theorem 1

Proof. For simplicity, we use $f_k(\boldsymbol{S}_{k-1})$ to replace $f_k^n(\boldsymbol{S}(k-1), \boldsymbol{\lambda}^n, \hat{\boldsymbol{d}}(k))$ here. First, let us define:

$$||G|| = \max_{\boldsymbol{S}_1, \boldsymbol{S}_2 \in G} ||\boldsymbol{S}_1 - \boldsymbol{S}_2||$$

$$||\nabla f|| = \max_{\boldsymbol{S} \in G, t=1,2,\ldots} ||\nabla f_k(\boldsymbol{S}_{k-1})||$$

Since f_k is convex in $\boldsymbol{S}$. Then we have,

$$f_k(\boldsymbol{S}^*) \geq \nabla f_k(\boldsymbol{S}_{k-1})(\boldsymbol{S}^* - \boldsymbol{S}_{k-1}) + f_k(\boldsymbol{S}_{k-1})$$
$$\Rightarrow f_k(\boldsymbol{S}_{k-1}) - f_k(\boldsymbol{S}^*) \leq \nabla f_k(\boldsymbol{S}_{k-1})(\boldsymbol{S}_{k-1} - \boldsymbol{S}^*) \quad \text{(A.1)}$$

Input: Demand distribution $\boldsymbol{D}$
Output: Location design $\boldsymbol{X}^*$, capacity initialization $\boldsymbol{S}^*$ and the initial assignment policy $\boldsymbol{Y}^*$.

Generate K demand samples $\boldsymbol{d}(k)$ independently according to the distribution of demand $\boldsymbol{D}$.
Arbitrarily sort the K samples into a sequence.
Solve a deterministic model [DM] with the average demand.
Set the iteration number $n = 0$ and initialize $\boldsymbol{X}^0, \boldsymbol{S}^0, \lambda_i^0$.
while $\min_{i\in I}\left\{\lambda_i^{n+1} - \lambda_i^n\right\} > \epsilon$ **do**
  for $k = 1, 2, \ldots, K$ **do**
    Solve the following primal problem given the demand scenario $\hat{\boldsymbol{d}}(k)$ and the Lagrangian dual multiplier $\boldsymbol{\lambda}^n$.
    Solve the dual problem.
    Update the capacity as $S_j^n(k) := \max\left\{S_j^n(k-1) - \gamma(k)\nabla_{S_j^n(k-1)} f(\cdot), 0\right\}$.
    Compute the average capacity $\bar{S}^n$ and expected capacity planning quantity $\bar{Y}_{ij}^n$ on each flow over K scenarios.
  end
  Update the dual multiplier $\boldsymbol{\lambda}^{n+1}$ as $\lambda_i^{n+1} := \lambda_i^n + \frac{1}{\sqrt{n}}(\beta_i \frac{\sum_{k=1}^K d_{jt}}{K} - \sum_{j\in J} Y_{ij}^n)$.
  Let $n = n + 1$.
end
Set $\boldsymbol{S}^* = \bar{\boldsymbol{S}}^n$, $\boldsymbol{X}^* = \bar{\boldsymbol{X}}^n$, and $\boldsymbol{Y}^* = \bar{\boldsymbol{Y}}^n$.

Algorithm 1: The pseudocode of OCO-based LR.

Input: Demand $\{\boldsymbol{d}(1), \boldsymbol{d}(2), \cdots, \boldsymbol{d}(T)\}$
Output: Adjusted capacity $\tilde{\boldsymbol{S}}^*$

Set $t = 1$, initial weight $\boldsymbol{w}(1) = \{1, 1, 1\}$.
for $t = 1, \ldots, T$ **do**
  Solve the sub-problem [Sub2(t)].
  for $k = 1, 2, 3$ **do**
    e update the weights as $w_k^+(t+1) = \max\left\{\frac{(t-1)w_k(t) + g_k(\cdot, \boldsymbol{d}(t)) - \tau_k}{t}, 0\right\}$.
  end
  Update $\tilde{\boldsymbol{S}}^* = \tilde{\boldsymbol{S}}^* + \Delta \boldsymbol{S}(T)$.
end

Algorithm 2: The pseudocode of adaptive dynamic allocation policy.

Let define $\boldsymbol{Z}_k := \boldsymbol{S}_{k-1} - \gamma(k)\nabla f_k(\boldsymbol{S}_{k-1})$. It is obvious that,

$$(\boldsymbol{Z}_k - \boldsymbol{S}^*)^2 \geq (\max\{\boldsymbol{Z}_k, 0\} - \boldsymbol{S}^*)^2 = (\boldsymbol{S}_k - \boldsymbol{S}^*)^2.$$

Therefore, we have,

$$\begin{aligned}(\boldsymbol{S}_k - \boldsymbol{S}^*)^2 &\leq (\boldsymbol{S}_{k-1} - \gamma(k)\nabla f_k(\boldsymbol{S}_{k-1}) - \boldsymbol{S}^*)^2 \\ &= (\boldsymbol{S}_{k-1} - \boldsymbol{S}^*)^2 - 2\gamma(k)(\boldsymbol{S}_{k-1} - \boldsymbol{S}^*)\nabla f_k(\boldsymbol{S}_{k-1}) \\ &\quad + \gamma^2(k)\nabla f_k^2(\boldsymbol{S}_{k-1})\end{aligned}$$

By transforming the above equation, we have,

$$(\boldsymbol{S}_{k-1} - \boldsymbol{S}^*)\nabla f_k(\boldsymbol{S}_{k-1}) \leq \frac{1}{2\gamma(k)}\left[(\boldsymbol{S}_{k-1} - \boldsymbol{S}^*)^2 - (\boldsymbol{S}_{k-1} - \boldsymbol{S}^*)^2\right] + \frac{\gamma(k)}{2}||\nabla f||^2 \tag{A.2}$$

Now, by summing we get:

$$\begin{aligned}&\text{Regret}(K) \\ &= \sum_{k=1}^K [f_k(\boldsymbol{S}_{k-1}) - f_k(\boldsymbol{S}^*)] \\ &\leq \sum_{k=1}^K [(\boldsymbol{S}^* - \boldsymbol{S}_{k-1})\nabla f_k(\boldsymbol{S}_{k-1})] \\ &\leq \sum_{k=1}^K \left\{\frac{1}{2\gamma(k)}\left[(\boldsymbol{S}_{k-1} - \boldsymbol{S}^*)^2 - (\boldsymbol{S}_{k-1} - \boldsymbol{S}^*)^2\right] + \frac{\gamma(k)}{2}||\nabla f||^2\right\} \\ &= \frac{1}{2\gamma(1)}(\boldsymbol{S}_0 - \boldsymbol{S}^*)^2 - \frac{1}{2\gamma(K)}(\boldsymbol{S}_K - \boldsymbol{S}^*)^2 \\ &\quad + \frac{1}{2}\sum_{k=2}^K \left(\frac{1}{\gamma(k)} - \frac{1}{\gamma(k-1)}\right)(\boldsymbol{S}_{k-1} - \boldsymbol{S}^*)^2 + \frac{||\nabla f||^2}{2}\sum_{k=1}^K \gamma(k) \\ &\leq ||G||^2\left\{\frac{1}{2\gamma(1)} + \frac{1}{2}\sum_{k=2}^K \left(\frac{1}{\gamma(k)} - \frac{1}{\gamma(k-1)}\right)\right\} + \frac{||\nabla f||^2}{2}\sum_{k=1}^K \gamma(k) \\ &= ||G||^2\frac{1}{2\gamma(K)} + \frac{||\nabla f||^2}{2}\sum_{k=1}^K \gamma(k)\end{aligned}$$

The first inequality follows (A.1). The second inequality follows (A.2). The second equality decomposes $\sum_{k=1}^K \left\{\frac{1}{2\gamma(k)}\left[(\boldsymbol{S}_{k-1} - \boldsymbol{S}^*)^2 - (\boldsymbol{S}_{k-1} - \boldsymbol{S}^*)^2\right]\right\}$ into three parts. The third equality uses the fact that $||\boldsymbol{S}_k - \boldsymbol{S}^*|| \leq ||G||$ and $\frac{1}{2\gamma(K)}(\boldsymbol{S}_K - \boldsymbol{S}^*)^2 \geq 0$

Since we define $\gamma(k) := \frac{1}{\sqrt{k}}$, we obtain,

$$\sum_{k=1}^K \gamma(k) = \sum_{k=1}^K \frac{1}{\sqrt{k}} \leq 1 + \int_{k=1}^K \frac{dt}{\sqrt{k}} = 2\sqrt{K} - 1$$

Therefore, we have,

$$\text{Regret}(K) \leq \frac{||G||^2}{2\sqrt{K}} + \frac{(2\sqrt{K} - 1)||\nabla f||^2}{2K} = \mathcal{O}\left(\frac{1}{\sqrt{K}}\right)$$

It is easy to obtain the desire results. □

Appendix B. The pseudocode of OCO-based LR

The detail procedure of OCO-based LR is presented as follows:

Appendix C. The pseudocode of adaptive dynamic allocation policy

The detail procedure of adaptive dynamic allocation policy is presented as follows:

Appendix D. Details of data

Details on facility candidates are summarized in Table D.8. We classify the sixty-six facility candidates into four types; let τ represent the facility type, and let $\tau = 1, 2, 3, 4$ correspond to a 3A hospital, a regional hospital, a regional CDC and a commercial testing institute. Assuming the fixed operational cost of a type-τ facility is $\tilde{f}_\tau$, then $\tilde{f}_1 = 200$, $\tilde{f}_2 = 150$, $\tilde{f}_3 = 100$, and $\tilde{f}_4 = 50$. Since there are 16 districts in Beijing, let γ_k be the average house price of district k ($k = 1, \cdots, 16$); then, the construction cost of facility type τ in district k is equal to $5.5 \cdot (\gamma_k/1000 + \tilde{f}_\tau/4)$, and the operational cost of facility type-τ in district k is $\gamma_k/160000 + \tilde{f}_\tau/160$. The longitudes and latitudes of reported nodes are collected from *Gaode*.

Table D.8
Details of the 66 facility candidates.

# Candidate	Type	District	Longitude	Latitude	f_j	a_{jt}
1	3A hospital	Changping	116.3293	40.0668	556.300	1.565
2	3A hospital	Chaoyang	116.4034	39.9729	829.500	1.870
3	3A hospital	Chaoyang	116.4545	39.9254	829.500	1.870
4	3A hospital	Chaoyang	116.3789	39.9952	829.500	1.870
5	3A hospital	Chaoyang	116.4583	39.9355	829.500	1.870
6	3A hospital	Chaoyang	116.4272	39.9739	829.500	1.870
7	3A hospital	Fengtai	116.3205	39.8382	727.700	1.755
8	3A hospital	Dongcheng	116.4173	39.9027	796.700	1.835
9	3A hospital	Dongcheng	116.4291	39.9310	796.700	1.835
10	3A hospital	Dongcheng	116.4270	39.9371	796.700	1.835
11	3A hospital	Fengtai	116.2954	39.8621	727.700	1.755
12	3A hospital	Fengtai	116.2778	39.8851	727.700	1.755
13	3A hospital	Fengtai	116.2538	39.8865	727.700	1.755
14	3A hospital	Haidian	116.3070	39.9409	696.800	1.720
15	3A hospital	Haidian	116.3011	39.9216	696.800	1.720
16	3A hospital	Haidian	116.3045	39.9244	696.800	1.720
17	3A hospital	Haidian	116.3240	39.9220	696.800	1.720
18	3A hospital	Haidian	116.2782	39.9070	696.800	1.720
19	3A hospital	Haidian	116.3600	39.9827	696.800	1.720
20	3A hospital	Haidian	116.3182	39.9001	696.800	1.720
21	3A hospital	Haidian	116.2643	39.9108	696.800	1.720
22	3A hospital	Xicheng	116.3513	39.9253	1101.900	2.175
23	3A hospital	Xicheng	116.3846	39.9244	1101.900	2.175
24	3A hospital	Dongcheng	116.4158	39.9128	796.700	1.835
25	3A hospital	Xicheng	116.3807	39.9320	1101.900	2.175
26	3A hospital	Xicheng	116.3544	39.9361	1101.900	2.175
27	3A hospital	Xicheng	116.3754	39.9442	1101.900	2.175
28	3A hospital	Xicheng	116.3905	39.8859	1101.900	2.175
29	3A hospital	Xicheng	116.3516	39.9193	1101.900	2.175
30	3A hospital	Xicheng	116.3624	39.8921	1101.900	2.175
31	Regional hospital	Pinggu	117.1058	40.1462	371.100	1.120
32	Regional hospital	Miyun	116.8704	40.3751	353.900	1.100
33	Regional hospital	Yanqing	115.9727	40.4629	401.900	1.155
34	Regional hospital	Mentougou	116.1017	39.9454	513.900	1.280
35	Regional hospital	Daxing	116.3352	39.7308	515.600	1.285
36	Regional hospital	Shunyi	116.6560	40.1282	484.300	1.250
37	Regional hospital	Shijingshan	116.2134	39.9064	527.200	1.295
38	Regional hospital	Huairou	116.6607	40.3171	365.500	1.115
39	Regional hospital	Tongzhou	116.6597	39.9013	479.800	1.245
40	Regional hospital	Fangshan	116.1404	39.7362	423.200	1.180
41	Regional CDC	Dongcheng	116.4115	39.9563	657.800	1.210
42	Regional CDC	Dongcheng	116.4096	39.8907	657.800	1.210
43	Regional CDC	Xicheng	116.3800	39.9528	963.000	1.550
44	Regional CDC	Chaoyang	116.4568	39.8740	690.600	1.245
45	Regional CDC	Haidian	116.2637	40.0494	557.900	1.095
46	Regional CDC	Fengtai	116.2788	39.8472	588.800	1.130
47	Regional CDC	Shijingshan	116.2082	39.9035	457.800	0.985
48	Regional CDC	Mentougou	116.1024	39.9525	444.400	0.970
49	Regional CDC	Fangshan	116.1506	39.7105	353.800	0.865
50	Regional CDC	Tongzhou	116.6525	39.9005	410.300	0.930
51	Regional CDC	Shunyi	116.6561	40.1295	414.800	0.935
52	Regional CDC	Daxing	116.3346	39.7319	446.100	0.970
53	Regional CDC	Changping	116.2323	40.2278	417.400	0.940
54	Regional CDC	Huairou	116.6314	40.3354	296.100	0.800
55	Regional CDC	Pinggu	117.1051	40.1473	301.700	0.810
56	Regional CDC	Miyun	116.8357	40.3806	284.400	0.790
57	Regional CDC	Yanqing	115.9631	40.4375	332.500	0.845
58	Regional CDC	Haidian	116.3787	39.9709	557.900	1.095
59	Commercial testing institutes	Daxing	116.5425	39.8008	376.700	0.660
60	Commercial testing institutes	Daxing	116.5065	39.7879	376.700	0.660
61	Commercial testing institutes	Fengtai	116.2805	39.8229	519.300	0.820
62	Commercial testing institutes	Chaoyang	116.5296	40.0248	621.100	0.935
63	Commercial testing institutes	Changping	116.2692	40.0987	347.900	0.625
64	Commercial testing institutes	Haidian	116.2347	39.9511	488.400	0.785
65	Commercial testing institutes	Haidian	116.1656	40.0637	488.400	0.785
66	Commercial testing institutes	Daxing	116.3021	39.6819	376.700	0.660

References

Albers, S. (2003). Online algorithms: A survey. *Mathematical Programming, 97*(1), 3–26.

Alem, D., Bonilla-Londono, H. F., Barbosa-Povoa, A. P., Relvas, S., Ferreira, D., & Moreno, A. (2021). Building disaster preparedness and response capacity in humanitarian supply chains using the social vulnerability index. *European Journal of Operational Research, in press*.

Arabani, A. B., & Farahani, R. Z. (2012). Facility location dynamics: An overview of classifications and applications. *Computers & Industrial Engineering, 62*(1), 408–420.

Arruda, E. F., Pastore, D. H., Dias, C. M., & Das, S. S. (2021). Modelling and optimal control of multi strain epidemics, with application to COVID-19. *PLoS ONE, 16*(9), e0257512.

Ballou, R. H. (1968). Dynamic warehouse location analysis. *Journal of Marketing Research, 5*(3), 271–276.

Basciftci, B., Ahmed, S., & Gebraeel, N.. Adaptive two-stage stochastic programming with an application to capacity expansion planning. arXiv preprint arXiv:1906.03513.
Basciftci, B., Ahmed, S., & Shen, S. (2021b). Distributionally robust facility location problem under decision-dependent stochastic demand. *European Journal of Operational Research, 292*(2), 548–561.
Bayram, V., Tansel, B. Ç., & Yaman, H. (2015). Compromising system and user interests in shelter location and evacuation planning. *Transportation Research Part B: Methodological, 72*, 146–163.
Bayram, V., & Yaman, H. (2018). Shelter location and evacuation route assignment under uncertainty: A benders decomposition approach. *Transportation Science, 52*(2), 416–436.
Beijing Municipal Health Commission (2020a). The list of COVID-19 testing facilities in Beijing. http://www.beijing.gov.cn/fuwu/bmfw/wsfw/ggts/202004/t20200421_1876070.html, Accessed April 15, 2020.
Beijing Municipal Health Commission (2020b). The list of COVID-19 testing facilities in Beijing. http://www.beijing.gov.cn/fuwu/bmfw/jhsyfwzdzx/jkbj/dt/202006/t20200623_1930777.html, Accessed June 23, 2020.
Beijing Municipal Health Commission (2021). The list of COVID-19 testing facilities in Beijing. http://www.beijing.gov.cn/fuwu/bmfw/wsfw/ggts/202101/t20210110_2210154.html, Accessed January 10, 2021.
Bellman, R. (1966). Dynamic programming. *Science, 153*(3731), 34–37.
Ben-Tal, A., El Ghaoui, L., & Nemirovski, A. (2009). *Robust optimization*. Princeton University Press.
Beraldi, P., & Bruni, M. E. (2009). A probabilistic model applied to emergency service vehicle location. *European Journal of Operational Research, 196*(1), 323–331.
Bertsekas, D. P., & Tsitsiklis, J. N. (1996). *Neuro-dynamic programming*. Athena Scientific.
CDC (2016). CDC releases detailed history of the 2014–2016 ebola response in MMWR. https://www.cdc.gov/media/releases/2016/p0707-history-ebola-response.html Accessed July 7, 2016.
CDC (2019). 2009 H1N1 pandemic (H1N1pdm09 virus). https://www.cdc.gov/flu/pandemic-resources/2009-h1n1-pandemic.html, Accessed June 11, 2010.
Cesa-Bianchi, N., & Lugosi, G. (2006). *Prediction, learning, and games*. Cambridge University Press.
Charles, A., Lauras, M., Wassenhove, L. N. V., & Dupont, L. (2016). Designing an efficient humanitarian supply network. *Journal of Operations Management, 47–48*, 58–70.
Chen, A. Y., & Yu, T.-Y. (2016). Network based temporary facility location for the emergency medical services considering the disaster induced demand and the transportation infrastructure in disaster response. *Transportation Research Part B: Methodological, 91*, 408–423.
China's State Council Information Office (2020). Full text: Fighting COVID-19: China in action. http://english.www.gov.cn/news/topnews/202006/07/content_WS5edc559ac6d066592a449030.html, Accessed Jun 07,2020.
CNN (2021). Global tally of confirmed coronavirus cases surpasses 100 million. https://edition.cnn.com/2021/01/26/world/coronavirus-100-million-cases-intl/index.html, Accessed January 26, 2021.
Dong, E., Du, H., & Gardner, L. (2020). An interactive web-based dashboard to track COVID-19 in real time. *The Lancet infectious diseases, 20*(5), 533–534.
Duong, V., Dussart, P., & Buchy, P. (2017). Zika virus in asia. *International Journal of Infectious Diseases, 54*, 121–128.
Dyer, O. (2021). Covid-19: Peru's official death toll triples to become world's highest. *BMJ, 373*, n1442.
Elçi, O., & Noyan, N. (2018). A chance-constrained two-stage stochastic programming model for humanitarian relief network design. *Transportation Research Part B: Methodological, 108*, 55–83.
Hong, X., Lejeune, M. A., & Noyan, N. (2015). Stochastic network design for disaster preparedness. *IIE Transactions, 47*(4), 329–357.
Jabbarzadeh, A., Fahimnia, B., & Seuring, S. (2014). Dynamic supply chain network design for the supply of blood in disasters: A robust model with real world application. *Transportation Research Part E: Logistics and Transportation Review, 70*, 225–244.
Jin, S., Ryan, S. M., Watson, J.-P., & Woodruff, D. L. (2011). Modeling and solving a large-scale generation expansion planning problem under uncertainty. *Energy Systems, 2*(3), 209–242.
Kılcı, F., Kara, B. Y., & Bozkaya, B. (2015). Locating temporary shelter areas after an earthquake: A case for turkey. *European Journal of Operational Research, 243*(1), 323–332.
Kınay, O. B., Kara, B. Y., Saldanha-da Gama, F., & Correia, I. (2018). Modeling the shelter site location problem using chance constraints: A case study for istanbul. *European Journal of Operational Research, 270*(1), 132–145.
Liberatore, F., Scaparra, M. P., & Daskin, M. S. (2011). Analysis of facility protection strategies against an uncertain number of attacks: The stochastic r-interdiction median problem with fortification. *Computers & Operations Research, 38*(1), 357–366.
Lin, J. T., Chen, T.-L., & Chu, H.-C. (2014). A stochastic dynamic programming approach for multi-site capacity planning in TFT-LCD manufacturing under demand uncertainty. *International Journal of Production Economics, 148*, 21–36.
Liu, K., Li, Q., & Zhang, Z.-H. (2019). Distributionally robust optimization of an emergency medical service station location and sizing problem with joint chance constraints. *Transportation Research Part B: Methodological, 119*, 79–101.
Lyu, G., Cheung, W.-C., Chou, M. C., Teo, C.-P., Zheng, Z., & Zhong, Y. (2019a). Capacity allocation in flexible production networks: theory and applications. *Management Science, 65*(11), 5091–5109.
Lyu, G., Cheung, W. C., Teo, C.-P., & Wang, H. (2019b). Multi-objective online ride–matching. *Available at SSRN 3356823*.
Malek, A., Abbasi-Yadkori, Y., & Bartlett, P. (2014). Linear programming for large-scale Markov decision problems. In *International conference on machine learning* (pp. 496–504). PMLR.
Marín, A., Martínez-Merino, L. I., Rodríguez-Chía, A. M., & Saldanha-da Gama, F. (2018). Multi-period stochastic covering location problems: Modeling framework and solution approach. *European Journal of Operational Research, 268*(2), 432–449.
Martínez-Costa, C., Mas-Machuca, M., Benedito, E., & Corominas, A. (2014). A review of mathematical programming models for strategic capacity planning in manufacturing. *International Journal of Production Economics, 153*, 66–85.
Meissner, J., & Senicheva, O. V. (2018). Approximate dynamic programming for lateral transshipment problems in multi-location inventory systems. *European Journal of Operational Research, 265*(1), 49–64.
Melo, M. T., Nickel, S., & Saldanha-Da-Gama, F. (2009). Facility location and supply chain management–a review. *European Journal of Operational Research, 196*(2), 401–412.
Mills, A. F., Argon, N. T., & Ziya, S. (2018). Dynamic distribution of patients to medical facilities in the aftermath of a disaster. *Operations Research, 66*(3), 716–732.
Mostajabdaveh, M., Gutjahr, W. J., & Salman, F. S. (2019). Inequity-averse shelter location for disaster preparedness. *IISE Transactions, 51*(8), 809–829.
Ni, W., Shu, J., & Song, M. (2018). Location and emergency inventory pre-positioning for disaster response operations: Min-max robust model and a case study of Yushu earthquake. *Production and Operations Management, 27*(1), 160–183.
Nickel, S., & Saldanha-da Gama, F. (2019). Multi-period facility location. In G. Laporte, S. Nickel, & F. Saldanha da Gama (Eds.), *Location Science* (pp. 303–326)). Cham: Springer International Publishing.
Nocedal, J., & Wright, S. J. (2006). *Numerical optimization. 2nd ed*. New York: Springer.
Noyan, N. (2010). Alternate risk measures for emergency medical service system design. *Annals of Operations Research, 181*(1), 559–589.
Parajuli, A., Kuzgunkaya, O., & Vidyarthi, N. (2021). The impact of congestion on protection decisions in supply networks under disruptions. *Transportation Research Part E: Logistics and Transportation Review, 145*, 102166.
Peng, C., Delage, E., & Li, J. (2020). Probabilistic envelope constrained multi-period stochastic emergency medical services location model and decomposition scheme. *Transportation Science, 54*(6), 1471–1494.
Powell, W. B. (2011). *Approximate dynamic programming: Solving the curses of dimensionality (2nd)*. Hoboken, NJ: John Wiley & Sons.
Powell, W. B. (2016). A unified framework for optimization under uncertainty. In *Optimization challenges in complex, networked and risky systems* (pp. 45–83). INFORMS.
Powell, W. B. (2019a). The next generation of optimization: A unified framework for dynamic resource allocation problems. In *Optimization in large scale problems* (pp. 47–52). Springer.
Powell, W. B. (2019b). A unified framework for stochastic optimization. *European Journal of Operational Research, 275*(3), 795–821.
Puterman, M. L. (2014). *Markov decision processes: Discrete stochastic dynamic programming*. John Wiley & Sons.
Queiroz, M. M., Ivanov, D., Dolgui, A., & Wamba, S. F. (2020). Impacts of epidemic outbreaks on supply chains: mapping a research agenda amid the COVID-19 pandemic through a structured literature review. *Annals of Operations Research*. in press
Rajagopalan, S., Singh, M. R., & Morton, T. E. (1998). Capacity expansion and replacement in growing markets with uncertain technological breakthroughs. *Management Science, 44*(1), 12–30.
Rawls, C. G., & Turnquist, M. A. (2010). Pre-positioning of emergency supplies for disaster response. *Transportation Research Part B: Methodological, 44*(4), 521–534.
Regnier, E. (2008). Public evacuation decisions and hurricane track uncertainty. *Management Science, 54*(1), 16–28.
Sabet, E., Yazdani, B., Kian, R., & Galanakis, K. (2020). A strategic and global manufacturing capacity management optimisation model: A scenario-based multi--stage stochastic programming approach. *Omega, 93*, 102026.
Shalev-Shwartz, S., et al. (2011). Online learning and online convex optimization. *Foundations and trends in Machine Learning, 4*(2), 107–194.
Shapiro, A., Dentcheva, D., & Ruszczyński, A. (2014). *Lectures on stochastic programming: Modeling and theory*. SIAM.
Shen, Z.-J. M., Zhan, R. L., & Zhang, J. (2011). The reliable facility location problem: Formulations, heuristics, and approximation algorithms. *INFORMS Journal on Computing, 23*(3), 470–482.
Sheu, J.-B. (2010). Dynamic relief-demand management for emergency logistics operations under large-scale disasters. *Transportation Research Part E: Logistics and Transportation Review, 46*(1), 1–17.
Shulman, A. (1991). An algorithm for solving dynamic capacitated plant location problems with discrete expansion sizes. *Operations Research, 39*(3), 423–436.
Silva, L., & Figueiredo Filho, D. (2021). Using Benford's law to assess the quality of COVID-19 register data in Brazil. *Journal of Public Health, 43*(1), 107–110.
Singh, K. J., Philpott, A. B., & Wood, R. K. (2009). Dantzig-Wolfe decomposition for solving multistage stochastic capacity-planning problems. *Operations Research, 57*(5), 1271–1286.
Snyder, L. V. (2006). Facility location under uncertainty: A review. *IIE Transactions, 38*(7), 547–564.
Tomasini, R., & Van Wassenhove, L. (2009). *Humanitarian logistics*. Springer.
Van Mieghem, J. A. (2003). Commissioned paper: Capacity management, invest-

ment, and hedging: Review and recent developments. *Manufacturing & Service Operations Management, 5*(4), 269–302.
Vatsa, A. K., & Jayaswal, S. (2021). Capacitated multi-period maximal covering location problem with server uncertainty. *European Journal of Operational Research, 289*(3), 1107–1126.
Velasquez, G. A., Mayorga, M. E., & Özaltın, O. Y. (2020). Prepositioning disaster relief supplies using robust optimization. *IISE Transactions, 52*(10), 1122–1140.
Wang, K.-J., & Nguyen, P. H. (2017). Capacity planning with technology replacement by stochastic dynamic programming. *European Journal of Operational Research, 260*(2), 739–750.
Wang, L. (2020). A two-stage stochastic programming framework for evacuation planning in disaster responses. *Computers & Industrial Engineering, 145*, 106458.
Wenjun, Shu, Jia, Song, & Miao (2018). Location and emergency inventory pre–positioning for disaster response operations: Min-max robust model and a case study of Yushu earthquake. *Production and Operations Management, 27*(1), 160–183.
Xu, Y., Qiu, X., Yang, X., Lu, X., & Chen, G. (2020). Disaster risk management models for rural relocation communities of mountainous southwestern China under the stress of geological disasters. *International Journal of Disaster Risk Reduction, 50*, 101697.
Yu, L., Yang, H., Miao, L., & Zhang, C. (2019). Rollout algorithms for resource allocation in humanitarian logistics. *IISE Transactions, 51*(8), 887–909.
Yu, L., Zhang, C., Yang, H., & Miao, L. (2018). Novel methods for resource allocation in humanitarian logistics considering human suffering. *Computers & Industrial Engineering, 119*, 1–20.
Yu, X., Ahmed, S., & Shen, S. (2021). On the value of multistage stochastic facility location with (or without) risk aversion. *Working paper*, 1–34.
Yu, X., & Shen, S. (2020). Multistage distributionally robust mixed-integer programming with decision-dependent moment-based ambiguity sets. *Mathematical Programming, 1–40*.
Zhang, Z.-H., & Li, K. (2015). A novel probabilistic formulation for locating and sizing emergency medical service stations. *Annals of Operations Research, 229*(jun), 813–835.
Zinkevich, M. (2003). Online convex programming and generalized infinitesimal gradient ascent. In *Proceedings of the 20th international conference on machine learning (ICML-03)* (pp. 928–936).